Edinburgh Research Explorer

Effect of pi-aromatic spacers on the magnetic properties and slow relaxation of double stranded metallacyclophanes with a Ln(III)-M-II-M-II-Ln(III) (Ln(III) = Gd-III, Dy-III, Y-III; M-II = Ni-II, Co-II) linear topology

OPEN ACCESS

Effect of π-aromatic spacers on the magnetic properties and slow relaxation of double stranded metallacyclophanes with a Ln^{III}-M^{II}-M^{II}-Ln^{III} (Ln^{III}= Gd^{III}, Dy^{III}, Y^{III}; M^{II}= Ni^{II}, Co^{II}) linear topology

Carlos Meseguer,[a] María A. Palacios,[a,] Antonio J. Mota,[a] Bouslav Drahos,[b] Euan K. Brechin,[c] R. Navarrete,[d] Jose M. Moreno,[a] Enrique Colacio[a,*]*

[a] Departamento de Química Inorgánica, Universidad de Granada, Av. Fuentenueva S/N, 18071 Granada (Spain)

[b] Department of Inorganic Chemistry, Faculty of Science, Palacky University Olomouc 17. listopadu 12, 771 46 Olomouc (Czech Republic)

[c] School of Chemistry. The University of Edinburgh, David Brewster Road, Edinburgh, EH9 3FJ (United Kingdom).

[d] Departamento de Química Inorgánica, Facultad de Farmacia, Universidad de Granada, Campus de Cartuja, 18071 Granada, Spain

Abstract

The coordination-driven self-assembly of two polydentate linear Schiff base ligands (either N,N-Bis(2-hydroxy-3-methoxy-benzyliden)-1,4-diaminobenzene, L2, or N,N-bis(2-hydroxy-3-methoxy-benzyliden)-1,5-diaminonaphthalene, L3) with two transition metal ions (M^{II}= Ni^{II} or Co^{II}) and two lanthanide ions (Ln^{III}= Gd^{III} or Dy^{III}) afforded seven linear M$_2$Ln$_2$ complexes of formulae [Ni$_2$Ln$_2$(L2)$_2$(CH$_3$CN)$_3$(H$_2$O)(NO$_3$)$_6$](CH$_3$CN)$_2$(H$_2$O) (Ln^{III}= Gd **1** and Dy **2**) and [M$_2$Ln$_2$(L3)$_2$(CH$_3$CN)$_4$(NO$_3$)$_6$](CH$_3$CN)$_x$ (M= Ni^{II}, Co^{II}; Ln= Dy^{III}, Gd^{III}, Y^{III}; x= 0-4) (**3-7**). Within the tetranuclear units of these complexes, two ligands coordinate through the N,O$_{phenoxide}$ donor sets to two M(II) ions, giving rise to M$_2$ metallacycles. In the case of complexes **1-2**, the Ni$_2$-metallacycle contains 14-members, where the Ni^{II} ions are bridged by para-phenylenediimine groups. In complexes **3-7**, the M$_2$-metallacycle consists of 18-members, where the transition metal ions are linked by naphthalenediimine bridging groups. At both sides of these metallacycles, the M^{II} ions are connected to Ln^{III} ions through phenoxido bridging groups. The analysis of the *dc* and *ac* magnetic properties of these complexes reveals that: (i) all the compounds exhibit weak ferromagnetic exchange interactions between the M^{II} and Ln^{III} ions through the bis(phenoxido) bridging groups and weak antiferromagnetic M^{II}−M^{II}

interactions transmitted by the acenediimine bridging groups; (ii) DFT calculations not only support the nature and magnitude of the magnetic exchange interactions, but also the polarization mechanism for the $M^{II}-M^{II}$ interactions through the acene bridging legends; (iii) The antiferromagnetic interaction for **1** is stronger than for **3**, which can be justified by the longer intermetallic Ni···Ni distance and α,α'-substitution for the latter; (iv) Complexes **2** and **4** show slow relaxation of the magnetization below 5 K at zero static magnetic field with U_{eff}/k_B values of 19 K and 15.9 K respectively, the higher U_{eff}/k_B value corresponding to the stronger J_{DyGd} coupling constant; (v) The change of $-\Delta S_m$ for the M_2Gd_2 complexes **1**, **3** and **6** has been analyzed by taking into account the values of their J and J_1 magnetic exchange interactions and single-ion anisotropies.

Introduction

Metallacycles in general, and metallacyclophanes, in particular, are of interest in supramolecular coordination chemistry not only because of their aesthetically pleasing architectures, but also because they can exhibit association or even interplay of interesting physical properties arising from each of their counterparts, that is to say metal ions and ligands [1]. These properties make them good candidates for potential applications in catalysis, biomedicine, luminescence, chemical sensing, molecular recognition and encapsulation, spintronics, information processing and storage, molecular magnetism and chirality [1-2].

The most common synthetic strategy to construct this kind of compound is the employment of linear or angular ligands partitioned into two binding domains well separated by spacers, so that each binding domain coordinates one or more metal ions. The coordination-driven self-assembly of metal ions or metal complexes (Lewis acids) and ligands or complexes acting "as ligands" (bearing Lewis-basic donors) leads to the metallacycle [1]. The features of both metal ions (oxidation state, coordination number, preferred geometry, stereochemical flexibility, lability and so forth) and ligands (denticity, type of donor atoms, ligand charge, and mutual orientation of the binding domains) are the most important factors behind the adoption of a specific structure. Using this strategy, numerous examples of metallacyclophane compounds have been obtained, most of them homonuclear in nature containing transition metal ions and, in a small number of cases, bearing 4f metal ions [3]. These compounds include helicates and

mesocates, where the ligands connecting different metal ions are twisted or non-twisted, respectively. It is worth mentioning that only a few examples of 3d-4f metallacycles have been reported so far, despite the fact that these compounds can exhibit, for example, interesting magnetic, luminescence and catalytic properties [4]. It should also be noted that some 3d-4f complexes behave as SMMs (Single-Molecule Magnet), which are nanomagnets that possess, like classical magnets, magnetic hysteresis and slow relaxation of the magnetization below a blocking temperature (T_B) [5]. Moreover, they also possess quantum properties, such as quantum tunneling of the magnetization (QTM) between up- and down-spin orientations, and quantum phase interference (QPI) between tunneling paths. These outstanding physical properties make them appropriate candidates for potential future applications in molecular spintronics, ultra-high density magnetic information storage, magneto-optics, and as qubits for quantum computing at the molecular level [6]. The origin of the SMM behaviour is tied to the existence of an energy barrier (U) that precludes magnetization reversal when the polarizing magnetic field is removed, such that the molecular magnetization can be blocked either parallel or antiparallel to the magnetic field (magnetic bistability) [5]. Because of this, these systems present slow relaxation between the two orientations of the magnetization. The magnetic anisotropy is the key factor in determining the height of the energy barrier and therefore the SMM properties [4]. Taking into account the above considerations, 3d-4f complexes containing anisotropic lanthanide ions could in principle be good candidates to exhibit SMM behaviour. Nevertheless, the SMM properties do not depend only on the single-ion anisotropy but also on the 3d-4f magnetic exchange interactions. In this regard, when the 3d-4f magnetic exchange interaction is strong enough, the exchange-coupled levels are well separated (thus circumventing the mixing of low-lying excited states in the ground state) and QTM is eliminated [7]. As QTM shortcuts the thermal barrier, its suppression leads to large effective energy barriers, hysteresis loops and long relaxation times. A paradigmatic case of the effect of the magnetic coupling on SMM behaviour is that of the butterfly-like $\{Cr^{III}_2Dy^{III}_2\}$ complexes, which show strong Cr^{III}-Dy^{III} interactions, U_{eff} values as high as 82 cm^{-1} and observable hysteresis loops up to 3.7 K [8]. In line with this strategy, we previously employed the Schiff base ligand, N, N$^{'}$-bis(3-methoxysalicylidene)-1,3-diaminobenzene (L1), which contains two dinucleating 3d-4f domains connected in the *meta* positions of a benzene ring, to prepare tetranuclear linear Ni$_2$Ln$_2$ complexes (Ln^{III} = Dy^{III}, Gd^{III}) (Scheme 1, top) [9]. These complexes can be described as dinuclear Ni^{II} metallacyclophanes with two appended lanthanide ions, each

linked to the Ni^{II} ions by phenoxide bridging groups. In keeping with other results previously reported for diphenoxo-bridged Ni^{II}-Gd^{III} complexes, the magnetic coupling between the Ni^{II} and Gd^{III} ions was found to be ferromagnetic in nature [4,10]. The interaction between the Ni^{II} ions was also ferromagnetic, justified by a spin polarization mechanism through the extended π-conjugated system of the *meta*-substituted aromatic ring [9]. This mechanism was also proposed to explain, for example, the magnetic exchange interaction observed in double-stranded dicopper(II) metallacycles containing oxamato donor groups separated by extended π-conjugated aromatic spacers [1j]. Here, it was assumed that the nearly perpendicular conformation between the two metal basal planes (where the dx^2-y^2 magnetic orbitals are located) and the plane of the aromatic spacer opens a π-pathway for the magnetic exchange interaction between the Cu^{II} ions. In such a mechanism, the nitrogen donor atoms hold the same spin density as the Cu^{II} ions due to the spin delocalization in the Cu-N bonds, whereas the carbon atoms of the aromatic spacer possess an alternating sign of spin density owing to spin polarization. The concomitant polarizations promoted by the unpaired electron of the Cu^{II} ions leads to the same or opposite sign of spin density on the Cu^{II} ions (ferromagnetic and antiferromagnetic interactions, respectively) when the number of the aromatic carbon atoms of the spacer is odd or even, respectively [1j]. In the case of the tetranuclear linear Ni_2Ln_2 complex (Scheme 1), the Ni^{II} ions exhibit an elongated octahedral geometry with the dx^2-y^2 magnetic orbital located in the equatorial coordination plane. As the equatorial coordination planes and the parallel planes of the benzene spacer are almost perpendicular, the spin polarization mechanism is operative [9]. Taking into account that the aromatic substituents are located in *meta*-positions, the number of carbons atoms between the nitrogen donor atoms is odd and this topology should lead to a ferromagnetic interaction, which agrees with the experimental result [9]. It is of interest to note that the Ni_2Dy_2 complex exhibited slow relaxation of the magnetisation and, consequently, SMM behaviour, whereas the Gd^{III} counterpart showed a significant magnetocaloric effect (MCE), which is characterized by the change of magnetic entropy (-ΔS_m) and adiabatic temperature (-ΔT_{ad}) triggered by the variation of the applied magnetic field. Specifically, the adiabatic demagnetization process leads to an increase in -ΔS_m and a decrease of -ΔT_{ad}, an effect that can be potentially used for cryogenic applications [11]. The observed MCE is a consequence of isotropic nature of the Gd^{III} (S= 7/2), the small magnetic anisotropy of the Ni^{II} ions, and the weak magnetic coupling between them. The

concomitant effect of both factors leads to high-spin multiple low-lying excited, field-accessible states, all of which contribute to the magnetic entropy of the system.
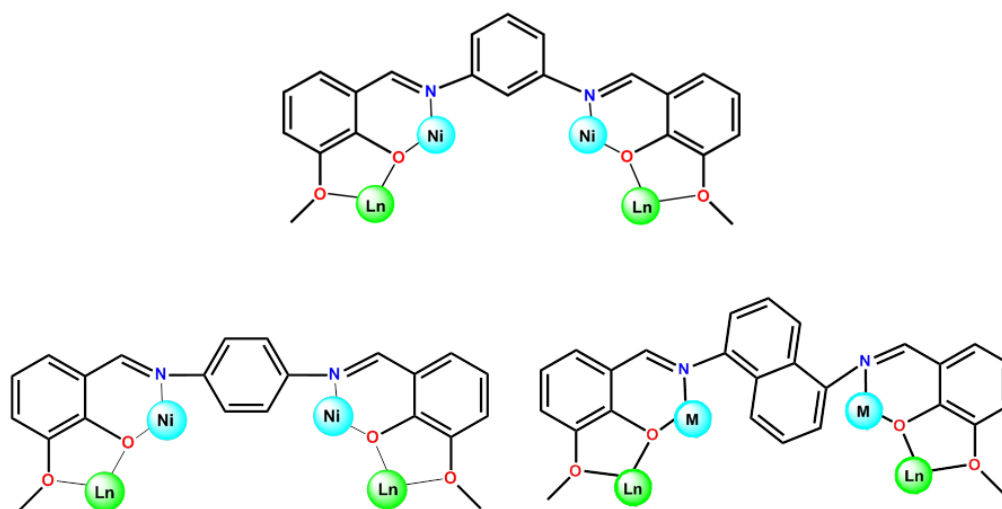
Scheme 1: Scheme of the L1 (up), L2 (down left) and L3 (down right) ligand systems, with the expected metal coordination.

The present paper is a continuation of this previous work and reports the design and preparation of two new tetranucleating ligands (L2 and L3) very closely related to L1, in which the 1,3-phenylene bridge in L1 has been replaced by either the 1,4-phenylene or 1,5-naphthalene counterparts (Scheme 1), as well as the preparation and magneto-structural characterization of their M_2Ln_2 complexes ($M^{II} = Ni^{II}$ or Co^{II}; $Ln^{III} = Dy^{III}$, Gd^{III} and Y^{III}). The aim of this work is four-fold: (i) to corroborate the antiferromagnetic nature of the Ni-Ni and Co-Co magnetic exchange interactions through a spin polarisation mechanism (there is an even number of aromatic carbon atoms between the metal ions); (ii) to analyse how the change of the phenylene ring by the naphthalene ring influences the magnitude of the Ni-Ni magnetic interaction; (iii) to check how the variation in the nature of the Ni-Ni interaction from ferromagnetic to antiferromagnetic affect the MCE or SMM properties, and (iv) to know how the substitution of Ni^{II} ions by Co^{II} ions modifies the MCE properties.

Experimental section

Materials

All chemicals were purchased from commercial sources and used without any further purification. Solvents were not dried prior to use.

Syntheses of ligands

Synthesis of N,N-bis(2-hydroxy-3-methoxy-benzyliden)-1,4-diaminobenzene(H_2L2) and N,N-bis(2-hydroxy-3-methoxy-benzyliden)-1,5-diaminonaphthalene(H_2L3).

Into a round bottomed flask containing a solution of *o*-vanillin (2.81 g, 18.5 mmol for H_2L2 and 7.7 g, 50.6 mmol for H_2L3) in 10 ml of MeOH were added 1,4-diaminobenzene (1g, 9.25 mmol) or 1,5-diamononaphthalene (4 g, 25.3 mmol) respectively, and the volume was completed to 25 ml with MeOH. The resulting reaction mixture was refluxed for 8h. After cooling, the formed precipitates were filtered off, washed with methanol and dried under vacuum.

For **H_2L2** Yield: 62%. Anal. Calcd. for $C_{22}H_{20}N_2O_4$: C, 70.20; H, 5.36; N, 7.44. Found: C, 69.87; H, 4.95; N, 7.88. IR (KBr, cm^{-1}): 3400, ν(OH); 2978, 2925, ν(CH); 1606ν(C=C); 1507, ν(CN); 1254 and 1199,ν(CO).^{1}H NMR ((CD$_3$)$_2$SO, ppm): 13.19 (s, 2H), 9.03 (s, 2H), 7.55 (s, 4H),7.26 (d, 2H), 7.14 (d, 2H), 6.93 (t, 2H), 3.83 (s, 6H).

For **H_2L3** Yield: 72%. Anal. Calcd. for $C_{26}H_{22}N_2O_4$: C, 73.23; H, 5.20; N, 6.57. Found: C, 72.87; H, 4.95; N, 6.88. IR (KBr, cm^{-1}): 3370, ν(OH); 1616, ν(C=C); 1464, ν(CN); 1251, ν(CO).^{1}H NMR ((CD$_3$)$_2$SO, ppm): 13.08 (s, 2H), 9.06 (s, 2H), 8.14 (d, 2H), 7.69 (t, 2H), 7.54 (d, 2H),7.38 (d, 2H), 7.21 (d, 2H), 6.98 (t, 2H), 3.87 (s, 6H).

Synthesis of complexes

Synthesis of [Ni$_2$Gd$_2$(L2)$_2$(CH$_3$CN)$_3$(H$_2$O)(NO$_3$)$_6$](CH$_3$CN)$_2$(H$_2$O) (1)

To a solution of H_2L2 (0.0475 g, 0.126 mmol) in 10 ml of acetonitrile were added sequentially, under heating and stirring, Ni(NO$_3$)$_2$·6H$_2$O (0.0365 g, 0.125 mmol), Gd(NO$_3$)$_3$·6H$_2$O (0.057 g, 0.126 mmol) and triethylamine (36 μL, 0.25 mmol). Stirring was maintained until all reactants had dissolved. The resulting yellow-green solution was filtered and allowed to evaporate at room temperature. Suitable crystals for X-ray diffraction formed after two days. Anal. Calc. For $C_{54}H_{55}Gd_2N_{15}Ni_2O_{28}$: C, 36.14; H, 3.07; N, 11.71. Found: C, 36.17; H, 3.59; N, 11.44. IR (KBr, cm^{-1}): 3400, ν(OH); 1609ν(C=C); 1560, ν(CN); 1399, ν(NO$_3^-$); 1232 and 1186, ν(CO).

Synthesis of [Ni$_2$Dy$_2$(L2)$_2$(CH$_3$CN)$_3$(H$_2$O)(NO$_3$)$_6$](CH$_3$CN)$_2$(H$_2$O) (2)

This compound was prepared following the same method as for compound **1** but using Dy(NO$_3$)$_3$·6H$_2$O (0.0565 g, 0.128 mmol) instead of Gd(NO$_3$)$_3$·6H$_2$O. After 48 h

suitable crystals for X-ray diffraction were obtained. Anal. Calc. For $C_{54}H_{55}Dy_2N_{15}Ni_2O_{28}$: C, 35.90; H, 3.05; N, 11.63. Found: C, 36.18; H, 3.26; N, 11.74. IR (KBr, cm^{-1}): 3400, ν(OH); 1613ν(C=C); 1560, ν(CN); 1403, ν(NO$_3^-$); 1235 and 1190, ν(CO).

Synthesis of [Ni$_2$Gd$_2$(L3)$_2$(CH$_3$CN)$_4$(NO$_3$)$_6$](CH$_3$CN)$_4$ (3)

To a solution of L3 (0.0278g, 0.0652 mmol) in acetonitrile (10 ml) were added sequentially, under stirring and heating (80 ºC), triethylamine (36 µL, 0.25 mmol), NiI$_2$ (0.0203 g, 0.065 mmol) and Gd(NO$_3$)$_3$·6H$_2$O (0.0325 g, 0.079 mmol). The reaction mixture was stirred and heated until all the reagents had dissolved. After 48 h, suitable crystals for X-ray diffraction were obtained by diffusion of diethyl ether into the mother liquid. Anal. Calc. For $C_{68}H_{64}Gd_2N_{18}Ni_2O_{26}$: C, 41.22; H, 3.26; N, 12.73. Found: C, 41.31; H, 3.21; N, 12.79.IR (KBr, cm^{-1}): 3400, ν(OH); 1611ν(C=C); 1559, ν(CN); 1404, ν(NO$_3^-$); 1210, ν(CO).

Synthesis of [Ni$_2$Dy$_2$(L3)$_2$(CH$_3$CN)$_4$(NO$_3$)$_6$](CH$_3$CN)$_3$ (4)

This compound was prepared following the same procedure as for **3** but using 0.058g of L3 (0.129 mmol), NiI$_2$ (0.040 g, 0.124 mmol) and Dy(NO$_3$)$_3$·6H$_2$O (0.057 g, 0.125 mmol) instead of Gd(NO$_3$)$_3$·6H$_2$O. After 48 h, green crystals suitable for X-ray diffraction were obtained by diffusion of diethyl ether into the mother solution. Anal. Calc. For $C_{66}H_{61}Dy_2N_{17}Ni_2O_{26}$: C, 40.64; H, 3.15; N, 12.21. Found: C, 41.01; H, 3.17; N, 12.56.IR (KBr, cm^{-1}): 3400, ν(OH); 1607ν(C=C); 1559, ν(CN); 1404, ν(NO$_3^-$); 1207, ν(CO).

Synthesis of [Ni$_2$Y$_2$(L3)$_2$(CH$_3$CN)$_4$(NO$_3$)$_6$](CH$_3$CN)$_8$ (5)

The synthesis of this compound was made following the same procedure as for **3** but using Y(NO$_3$)$_3$·6H$_2$O (0.0253 g, 0.0661 mmol) instead of Gd(NO$_3$)$_3$·6H$_2$O. After 24 h, green crystals suitable for X-ray diffraction were obtained by diffusion of the mother liquid with diethyl ether. Anal. Calc. For $C_{76}H_{76}Y_2N_{22}Ni_2O_{26}$: C, 45.44; H, 3.81; N, 15.34. Found: C, 45.54; H, 3.78; N, 15.02.IR (KBr, cm^{-1}): 3400, ν(OH); 1609ν(C=C); 1540, ν(CN); 1404, ν(NO$_3^-$); 1245, ν(CO).

Synthesis of [Co$_2$Gd$_2$(L3)$_2$(CH$_3$CN)$_2$(NO$_3$)$_6$](CH$_3$CN)$_5$ (6)

To a solution of L3 (0.058g, 0.129 mmol) in acetonitrile (10 ml) were added sequentially, under stirring and heating (80 °C), $Co(NO_3)_2 \cdot 6H_2O$ (0.037 g, 0.127 mmol), $Gd(NO_3)_3 \cdot 6H_2O$ (0.060 g, 0.133 mmol) and triethylamine (36 μL, 0.25 mmol). The reaction mixture was stirred and heated until all the reagents had dissolved. After 48 h, orange crystals suitable for X-ray diffraction were obtained by diffusion of diethyl ether into the mother liquid. Anal. Calc. For $C_{70}H_{67}Gd_2N_{19}Co_2O_{26}$: C, 41.57; H, 3.34; N, 13.16. Found: C, 41.69; H, 3.28; N, 12.99. IR (KBr, cm^{-1}): 3400, ν(OH); 1611ν(C=C); 1562, ν(CN); 1404, ν(NO_3^-); 1210, ν(CO).

Synthesis of $[Co_2Dy_2(L3)_2(CH_3CN)_2(NO_3)_6](CH_3CN)_2$ (7)

The method followed to prepare this compound was the same as for **6** but using $Dy(NO_3)_3 \cdot 6H_2O$ (0.057 g, 0.125 mmol) instead of $Gd(NO_3)_3 \cdot 6H_2O$. After 48 h, suitable orange crystals for X-ray diffraction were obtained by diffusion of diethyl ether into the mother solution. Anal. Calc. For $C_{64}H_{58}Dy_2N_{16}Co_2O_{26}$: C, 40.24; H, 3.06; N, 11.73. Found: C, 40.33; H, 2.98; N, 11.79. IR (KBr, cm^{-1}): 3400, ν(OH); 1608ν(C=C); 1556, ν(CN); 1407, ν(NO_3^-); 1207, ν(CO).

Physical Measurements

Elemental analyses were carried out at the "Centro de Instrumentación Científica" (University of Granada) on a Fisons-Carlo Erba analyser model EA 1108. The IR spectra on powdered samples were recorded with a ThermoNicolet IR200FTIR by using KBr pellets and ^1H NMR spectra on a Bruker ARX400 spectrometer.

Single-Crystal Structure Determination

Suitable crystals of compounds were mounted on a glass fibre and used for data collection on a Bruker AXS Smart Apex CCD (**1-2**) and Rigaku Oxford Diffraction SuperNova diffractometer (**3-7**) at 100 K using graphite monochromated MoKα radiation (λ = 0.71073 Å). Unit-cell parameters were determined and refined on all observed reflections using APEX2 software [12]. Correction for Lorentz polarization and absorption were applied by SAINT and SADABS programs, respectively [13-14]. The structures were solved by direct methods and refined by full-matrix least-squares on F^2 using the SHELX software suite [15] and Olex2 [16]. Hydrogen atom positions were calculated and isotropically refined as riding models to their parent atoms. Details of data collections and refinements are given in Table 1.

Table 1: Crystallographic data and structural refinement details for compounds **1-7**.

Compound	1	2	3	4	5	6	7
chemical formula	$C_{54}H_{55}N_{15}O_{28}Gd_2Ni_2$	$C_{54}H_{55}N_{15}O_{28}Dy_2Ni_2$	$C_{68}H_{64}Gd_2N_{18}Ni_2O_{26}$	$C_{66}H_{61}Dy_2N_{17}Ni_2O_{26}$	$C_{76}H_{76}N_{22}Ni_2O_{26}Y_2$	$C_{70}H_{67}Co_2Gd_2N_{19}O_{26}$	$C_{64}H_{58}Co_2Dy_2N_{16}O_{26}$
M/gmol^{-1}	1794.05	1804.55	1981.29	1950.73	2008.82	2022.78	1910.12
cryst syst	orthorhombic	orthorhombic	triclinic	triclinic	monoclinic	monoclinic	triclinic
space group	$P2_1/2_1/2_1$	$P2_1/2_1/2_1$	P-1	P-1	$P2_1/c$	$P2_1/n$	P-1
a/ Å	17.1683(5)	17.151(3)	11.6700(3)	11.7205(6)	12.2112(8)	21.7530(4)	11.7687(7)
b/ Å	18.7509(5)	18.671(4)	15.9458(3)	15.9129(6)	15.9604(7)	16.0410(3)	15.9986(5)
c/ Å	20.0391(5)	20.033(4)	21.3630(4)	21.3631(6)	21.4821(7)	22.6237(5)	21.3753(9)
α/deg	90	90	91.2262(14)	90.844(3)	90	90	90.519(3)
β/deg	90	90	102.3043(17)	102.803(3)	98.331(4)	99.798(2)	102.930(4)
γ/deg	90	90	94.6488(16)	96.018(4)	90	90	96.164(4)
V/ Å^3	6451.0(3)	6415(2)	3868.26(13)	3860.9(3)	4142.6(4)	7779.2(3)	3897.6(3)
Z	4	4	2	2	2	4	2
ρ(g cm^{-3})	1.847	1.868	1.701	1.678	1.610	1.727	1.628
μ(mm^{-1})	2.703	2.980	12.238	11.486	1.928	2.195	2.399
Θ_{min} (º)	2.58	2.35	3.43	3.44	3.132	3.389	2.933
Θ_{max} (º)	30.56	28.33	76.11	67.07	20.814	29.356	21.966
Independent Reflections	17385	19392	16037	13763	4318	20627	9503
Reflections Used	9657	9951	14000	10118	3665	16341	8410
R_{int}	0.0351	0.0275	0.0728	0.0863	0.0611	0.0533	0.1131
Parameters	936	898	1058	1058	436	1001	960
Restraints	0	36	76	85	490	9	453
R1^a [I>2σ(I)]	0.0437	0.0351	0.0658	0.0898	0.1289	0.0653	0.1302
R1 (all data)	0.0646	0.0386	0.0736	0.1134	0.1422	0.0843	0.1397
wR2^a [I>2σ(I)]	0.1239	0.0904	0.1700	0.2421	0.3312	0.1387	0.3271
wR2 (all data)	0.1647	0.0935	0.1772	0.2658	0.3437	0.1446	0.3329
Goodness of fit on F^2	1.364	0.975	1.048	1.021	1.053	1.104	1.173

Magnetic Properties

Magnetic measurements on powdered crystalline samples of **1-7** were carried out with Quantum Design PPMS Dynacool with the VSM option and Quantum Design SQUID MPMS XL-5/XL-7 (T = 1.9–300 K at B = 0.1 T; B = 0–5 T at T = 2-7 K). Alternating-current (ac) susceptibility measurements under zero or applied static field were performed using an oscillating ac field of 3.5 Oe and ac frequencies ranging from 1 to 1500 Hz. The magnetic data were corrected for sample holder signal and for diamagnetic susceptibility.

Results and discussion

The Schiff base ligands N,N-bis(2-hydroxy-3-methoxy-benzyliden)-1,4-diaminobenzene (H$_2$L2) and N,N-bis(2-hydroxy-3-methoxy-benzyliden)-1,5-diaminonaphthalene (H$_2$L3) were prepared in reasonable yield by condensation of the corresponding aromatic diamine

with *o*-vanillin in 1:2 molar ratio. These linear ligands are partitioned in two NOO' tridentate bridging coordination domains well separated by 1,4-phenyl and 1,5-naphthyl spacers. The NO donor part of these coordination domains prefers transition metal ions whereas the OO' part has a tendency to coordinate lanthanide ions. Therefore, the coordination-driven self-assembly of two of these ligands with two transition metal ions (M^{II} = Ni^{II} or Co^{II}) and two lanthanide ions (Gd^{III} or Dy^{III}) is expected to afford M_2Ln_2 complexes where the M^{II} ions are connected by either phenylendiimine or naphtylendiimine bridges and the M^{II} and Ln^{III} ions by phenoxide bridging groups. In keeping with this, the reaction between H_2L2 and $Ni(NO_3)_2 \cdot 6H_2O$ and subsequent reaction with $Ln(NO_3)_3$ and triethylamine in acetonitrile solution using a 1:1:1:2 molar ratio afforded the tetranuclear Ni_2Ln_2 complexes $[Ni_2Ln_2(L2)_2(CH_3CN)_3(H_2O)(NO_3)_6](CH_3CN)_2(H_2O)$ (Ln^{III}= Gd **1** and Dy **2**). Following the same procedure but using the ligand H_2L3 and NiI_2 allowed the preparation of the complexes $[Ni_2Ln_2(L3)_2(CH_3CN)_4(NO_3)_6](CH_3CN)_n$ (Ln^{III} = Gd, n = 4 for **3** and Dy, n= 3 for **4**) and $[Ni_2Y_2(L3)_2(CH_3CN)_4(NO_3)_6]](CH_3CN)_8$ (**5**). The use, in the same reactions conditions, of H_2L3 and $Co(NO_3)_2 \cdot 6H_2O$ and further diffusion of diethyl ether into the mother solution yielded the complexes $[Co_2Ln_2(L3)_2(CH_3CN)_2(NO_3)_6](CH_3CN)_n$ (Ln^{III} = Gd, n= 6 for **6** and Dy, n= 2 for **7**).

Crystal structures

$[Ni_2Ln_2(L2)_2(CH_3CN)_3(H_2O)(NO_3)_6](CH_3CN)_2(H_2O)$ (Ln= Dy^{III}, Gd^{III}) (1-2)

Single-crystal X-ray diffraction studies reveal that compounds **1** and **2** are isostructural and therefore we will describe here the structure of **2** as a representative example to illustrate the common features of these two complexes. The molecular structure of **2** is shown in Figure 1, and selected bond distances and angles for **1** and **2** are given in Table S1.
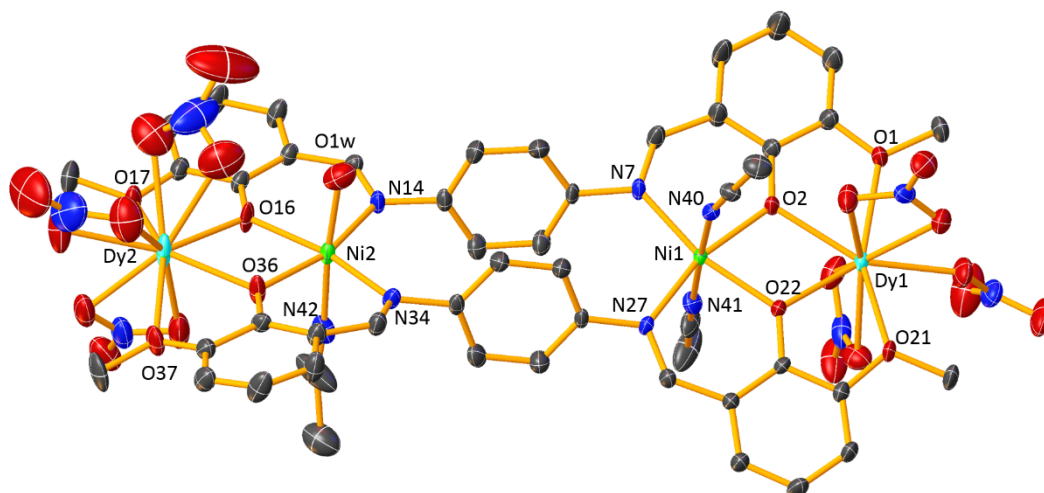
*Figure 1: Perspective view of the structure of **2**. Hydrogen atoms and non-coordinated solvent molecules are omitted for clarity.*

The X-ray structure of **2** (Figure 1) consists of linear, neutral tetranuclear Ni_2Dy_2 molecule with C_1 symmetry along with solvent molecules of crystallization (one water and two acetonitrile molecules). Within the tetranuclear unit, two ligand strands coordinate through the $N,O_{phenoxide}$ donor sets to two Ni^{II} ions, giving rise to a 14-membered Ni_2 metallacycle. In addition, at both sides of this metallacycle, the Ni^{II} ions are connected to Dy^{III} ions through phenoxido bridging groups, so that the latter ions are coordinated by the $O_{phenoxido}O_{methoxy}$ donor sets of the ligand. This disposition of metal ions leads to Ni⋯Ni, Ni1⋯Dy1, Ni2⋯Dy2 and Dy⋯Dy distances of 8.116(2), 3.5276(10), 3.5709(11) and 15.212(3) Å, respectively. The Dy-O-Ni bridging angles are 107.5(2) and 108.18(19)° for the Dy1-($O_{phenoxido}$)-Ni1 unit and 108.9(2) and 109.6(2)° for the Dy2-($O_{phenoxido}$)-Ni2 counterpart.

The Ni^{II} ions exhibit a distorted octahedral coordination geometry, in which the N,O-donor atoms of the two $L2^{2-}$ bridging ligands occupy equatorial positions, with two acetonitrile molecules on Ni1 and one water and one acetonitrile molecule on Ni2 placed in the axial positions. The $Ni-O_{phenoxido}$ and $Ni-N_{acetonitrile}$ bond distances are in the range 2.060(3) to 2.088(4) Å, whereas the $Ni-N_{imine}$ and $N-O_{water}$ bond distances are slightly larger, with values in the range 2.091(3)-2.128(3) Å for the former and 2.106(4) for the latter.

The Dy^{III} ions show $Dy1O_9$ and $Dy2O_{10}$ coordination spheres, which are formed by the coordination of the oxygen atoms belonging to the phenoxido and methoxy groups

of the ligands and the nitrate oxygen atoms (five oxygen atoms belonging to one monodentate and two bidentate nitrate anions in the case of Dy1, and six oxygen atoms pertaining to three bidentate nitrate anions in the case of the Dy2 ion). The Dy-O bond distances for the donor oxygen atoms belonging to the phenolate groups are slightly shorter (2.291(3)-2.310(4) Å) than those belonging to the nitrate and methoxy groups (2.340(3)-2.680(7) Å).

The $Ni(O_{phenoxido})_2Dy$ fragments are almost planar with dihedral angles between the O-Ni-O and O-Dy-O planes of 5.7(2) and 3.1(3)° for $Ni1(O_{phenoxido})_2Dy1$ and $Ni2(O_{phenoxido})_2Dy2$ bridging fragments, respectively. The dihedral angle between the mean planes of these two $Ni(O_{phenoxido})_2Dy$ moieties is 22.2(3)°. The mean planes of the phenyl rings of the spacers are almost parallel with a dihedral angle of 3.4(2)° between each other and a centroid to centroid distance of 3.266(4) Å, thus indicating the existence of an important π-π stacking interaction. The dihedral angles between these planes and the $Ni1(O_{phenoxido})_2Dy1$ and $Ni2(O_{phenoxido})_2Dy2$ are 60.3(2) and 82.6(3)°, respectively.

Finally, the coordinated water molecule in both **1** and **2** is involved in intramolecular hydrogen bonding with the one of the oxygen atoms of the coordinated nitrate anions with donor-acceptor distances of 2.640(14) and 2.998(16) Å for **1** and 2.633(14) Å for **2**. Moreover, the coordinated water molecule in **1** also forms a hydrogen bond with a non-coordinated acetonitrile molecule (donor-acceptor distance 2.640(13) Å), whereas in **2** the hydrogen bond is established with a non-coordinated water molecule (donor-acceptor distance 2.735(16) Å).

$[M_2Ln_2(L3)_2(CH_3CN)_4(NO_3)_6](CH_3CN)_x$ (M=Ni^{II}, Co^{II}; Ln=Dy^{III}, Gd^{III},Y^{III}; X = 0-8) (3-7)

Although complexes **3**, **4** and **7** crystallize in the triclinic space group *P-1* and complexes **5** and **6** in the monoclinic $P2_1/c$ and $P2_1/n$ space groups, respectively, the general structural features of all three are similar. In view of this, we will describe only the structure of **4** as a representative example to illustrate the common characteristics of this family of complexes. We will thereafter highlight the main differences between them. The molecular structure of **4** is shown in Figure 2, with selected bond lengths and angles for **3-7** given in Table S2.
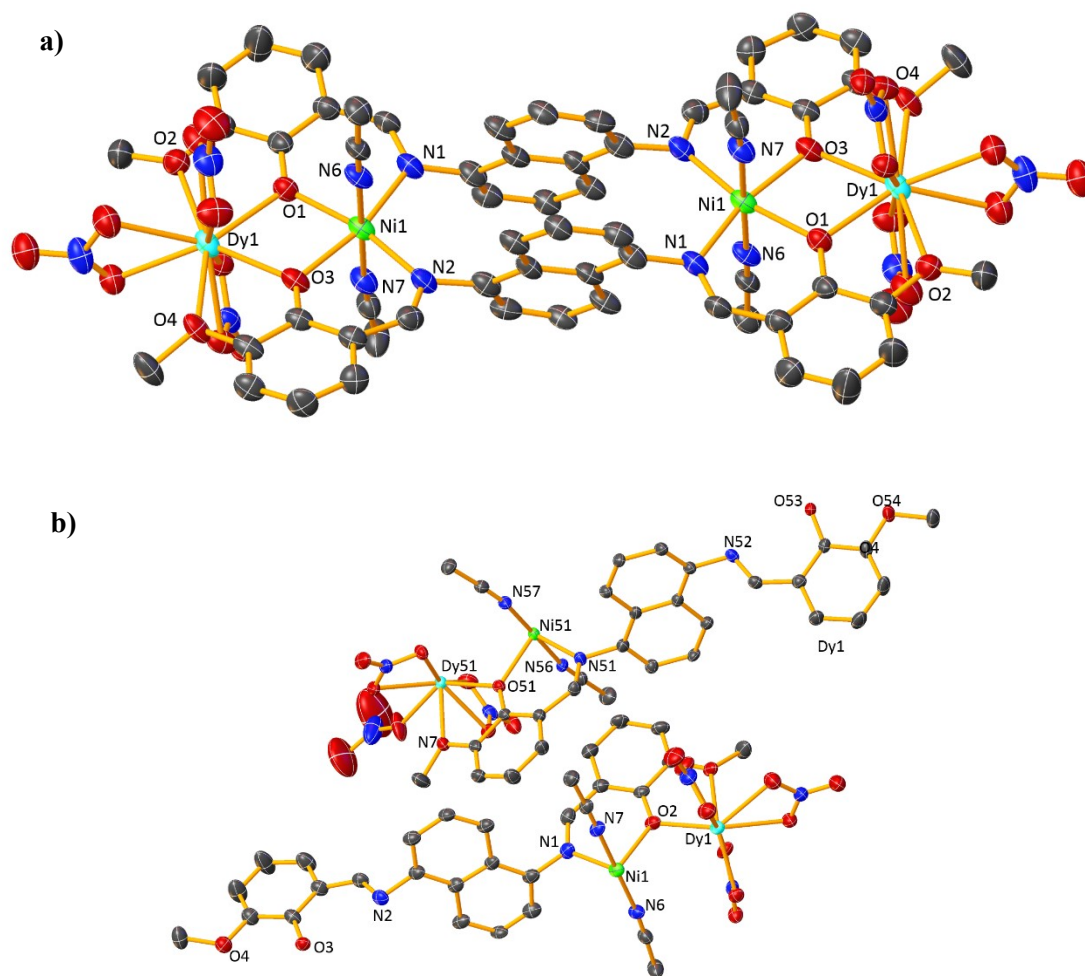
*Figure 2: a) Perspective view of the structure of **4**. b) Asymmetric unit for **4**. Hydrogen atoms and non-coordinated solvent molecules are omitted for clarity.*

The structure of **4** contains two very similar, but different linear tetranuclear Ni_2Dy_2 molecules with C_i symmetry and three acetonitrile molecules of crystallization. Each of the neutral tetranuclear Ni_2Dy_2 molecules is made of an 18-membered Ni_2 metallacycle bearing two di(μ-naphthalendiimine) bridges. Moreover, the Ni^{II} ions at both ends of the metallacycle are connected to Dy^{III} ions through diphenoxido-bringing groups, leading ultimately to the Dy-Ni-Ni-Dy linear arrangement of metal ions with $Ni\cdots Ni$, $Ni1\cdots Dy1$, $Ni2\cdots Dy2$ and $Dy\cdots Dy$ distances of 8.713(3), 3.538(2), 3.533(2) and 15.7707(15) Å, respectively.

The Ni^{II} ions exhibit a distorted octahedral coordination geometry, with the equatorial plane formed by two *cis*-imine nitrogen atoms and two phenolate oxygen atoms belonging to two fully deprotonated bis(tridentate) $L3^{2-}$ bridging ligands. The axial

positions are occupied by two nitrogen atoms of two acetonitrile molecules. The Ni-N_{imine} and Ni-O_{phen} bond distances are in the range of 2.082(11)-2.129(8) and 2.052(8)-2.091(8) Å, respectively, whereas the Ni-N axial bond distances range between 2.063(9) and 2.101(10) Å (Table S2).

In one of the Ni_2Dy_2 molecules, the Dy^{III} ion exhibits a non-symmetric DyO_{10} coordination sphere, which is made of two oxygen atoms belonging to the diphenoxido bridging groups, two oxygen atoms from the methoxy groups and six oxygen atoms belonging to three bidentate nitrate anions. In the other Ni_2Dy_2 molecule, the Dy^{III} coordination sphere is built by the same atoms of the ligands and by five oxygen atoms belonging to two bidentate and one-monodentate nitrate anions, ultimately leading to a DyO_9 coordination environment. The Dy-$O_{phenoxido}$ bond distances, in the range of 2.283(6)-2.315(7) Å, are shorter than the Dy-$O_{nitrate}$ and Dy-$O_{methoxy}$ bond lengths which are in the ranges 2.293(11)-2.583(12) and 2.464(8)-2.499(10) Å, respectively. The Ni(μ-$O_{phenoxido}$)$_2$Dy dinuclear fragments of the two Ni_2Dy_2 molecules are essentially planar, with dihedral angles between the O-Ni-O and O-Dy-O mean planes of 2.6(4) and 7.4(3)° and with Ni-O-Dy bridging angles of 108.6(3) and 107.3(3)° for a molecule and 108.6(3) and 107.1(3)° for the other. The naphthyl aromatic rings of the two Ni_2Dy_2 molecules are planar and strictly parallel to each other, with centroid-to-centroid distances of 3.331(8) and 3.359(6) Å. These planes form, with the mean plane of the Ni(μ-$O_{phenoxido}$)$_2$Dy fragments, dihedral angles of 79.0(3) and 76.8(2)°, thus indicating a strong π-π staking interaction between the naphthyl rings.

It is worth noting that compound **6** shows a significant difference with complexes **3**, **4** and **7**. That is, whereas the naphthyl rings of the two strands in **3**, **4** and **7** are parallel and coincident, those of **6** are almost parallel albeit slightly turned towards each other. The arrangement of naphthyl rings in **6** leads to a disposition of the imine nitrogen atoms forming the equatorial plane of the Co^{II} coordination sphere, in which, in contrast to that found for complexes **3**, **4** and **7**, one of these nitrogen atoms is above the equatorial plane and the other below this plane. This disposition gives rise to a significant distortion of the Co^{II} octahedral geometry (see Figure 3). In fact, continuous shape measurements using the SHAPE software [17] indicate that the Co^{II} coordination sphere in **6** is more distorted from octahedral geometry than the Ni^{II} coordination sphere in complexes **3** and **4** and the Co^{II} coordination sphere in **7** (see Tables S3-S5).
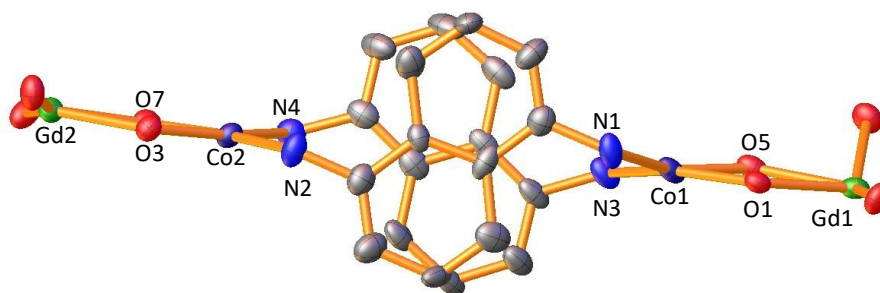
*Figure 3.- Non-eclipsed disposition of the acene rings in compound **6**.*

Finally, it is worth mentioning that the tetranuclear M_2Ln_2 molecules of complexes **3-7** are well isolated, because neither hydrogen bonds interactions nor $\pi\cdots\pi$ intermolecular staking interactions are observed in their corresponding extended structures.

Magnetic properties

Ni_2Ln_2 (Ln^{III}= Gd, Dy)

Let us begin with the analysis of the magnetic properties of the Gd^{III} compounds **1** and **3**. The temperature dependence of the $\chi_M T$ product for **1** is shown in Figure 4. At room temperature, the $\chi_M T$ value (20.82 cm³ K mol⁻¹) is somewhat larger than that expected for two non-interacting Ni^{II} ions ($S = 1$) and two non-interacting Gd^{III} ions ($S = 7/2$), assuming a g-value of 2.0 (17.75 cm³ K mol⁻¹). The deviation of the experimental $\chi_M T$ value from the expected value is due to both the second-order spin-orbit coupling for the Ni^{II} ions (λ is negative and therefore increases the expected $\chi_M T$ value), and the existence of a significant ferromagnetic interaction between Ni^{II} and Gd^{III} ions. On lowering temperature, the $\chi_M T$ product steadily increases to reach a maximum value of 21.68 cm³ K mol⁻¹ at 10 K. Below this temperature, $\chi_M T$ sharply decreases down to 2 K, reaching a value of 10.58 cm³ K mol⁻¹.
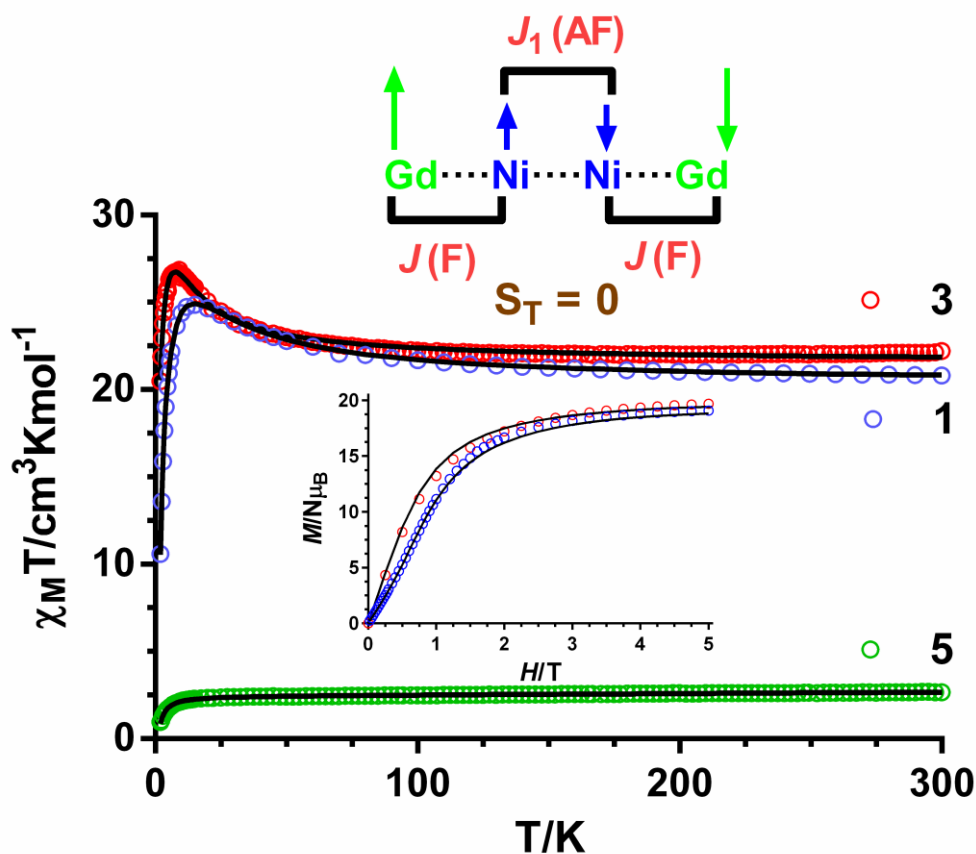
*Figure 4: Temperature dependence of the $\chi_M T$ product and field dependence of the magnetization at 2 K (inset bottom) for **1**, **3** and **5**. The solid lines represent the best fit of the magnetic data. Coupling scheme for Ni-Gd and Ni-Ni interactions (inset top)*

The increase of the $\chi_M T$ product from 300 to 10 K is due to the ferromagnetic interactions between Ni^{II} and Gd^{III} ions through the phenoxide bridging groups, whereas the decrease below 10 K is due to both the Ni^{II}-Ni^{II} antiferromagnetic interactions through the diphenylenediimine groups and the zero field splitting of Ni^{II} ions. The magnetic properties of **1** were modelled with the following Hamiltonian:

$$H = -J(\hat{S}_{Ni1}\hat{S}_{Gd1} + \hat{S}_{Ni2}\hat{S}_{Gd2}) - J_1(\hat{S}_{Ni1}\hat{S}_{Ni2}) + \sum_{i=1}^{2} D_{Nii}(\hat{S}_{zNii}^2 - 2/3) +$$
$$\mu_B H \left[\sum_{i=1}^{2} g_{Nii}\hat{S}_{Nii} + \sum_{i=1}^{2} g_{Gdi}\hat{S}_{Gdi}\right] \quad \text{(equation 1)}$$

where J and J_1 represent the magnetic exchange coupling between Ni^{II} and Gd^{III} through the diphenoxido bridging groups, and between Ni^{II} ions through the phenylenediimine bridging groups, respectively. D_{Nii} is the axial zero field-splitting parameter (ZFS) of the Ni^{II} ions, and the last term of the equation corresponds to the

Zeeman Effect.

The simultaneous fit of the temperature dependence of the $\chi_M T$ product and the field dependence of the magnetisation at 2 K with the above Hamiltonian using the PHI program [18] (in order to avoid over-parameterisation, we assumed an average g value for all the cations and the same ZFS parameter for both Ni^{II} ions) led to the following parameters: J = +4.1 cm^{-1}, J_1 = -2.0 cm^{-1}, g = 2.14, $|D|$ = 8.7 cm^{-1} and R = 3x10^{-5} (R = $\Sigma[(\chi_M T)_{exp.}-(\chi_M T)_{calcd.}]^2/\Sigma((\chi_M T)_{exp})^2)$. If D is fixed to zero the following values are obtained, J = +4.2 cm^{-1}, J_1 = -2.6 cm^{-1}, g = 2.14 and R = 1x10^{-5}. As can be observed, when D = 0, J and g values remain virtually constant, whereas J_1 slightly increases. As D and J_1 produce similar effects on the $\chi_M T$ product (a decrease at low temperature), the J_1 values obtained from the second fitting procedure can be considered as the higher limit of this magnetic exchange constant. In order to support unambiguously the antiferromagnetic nature of the Ni^{II}-Ni^{II} interactions we attempted to prepare the isostructural Ni_2Y_2 complex. However, all attempts to obtain this complex in pure form failed. It is worth noting that the field dependence of the magnetization at low fields and at 2 K shows a sigmoidal shape (Figure 4), which is a hallmark of the existence of antiferromagnetic Ni⋯Ni interactions.

The $\chi_M T$ product for **3** at room temperature (22.21 cm^3 K mol^{-1}) is higher than expected for two Ni^{II} and two Gd^{III} magnetically isolated ions (S_{Gd} = 7/2, S_{Ni} = 1, g_{Gd} = 2.0, g_{Ni} = 2.0), but still close to the upper limit calculated taking into account both the second-order spin orbit of the Ni^{II} ions and, as in the case of **1**, a ferromagnetic interaction between Ni^{II} and Gd^{III} ions. When the temperature is lowered from room temperature, the $\chi_M T$ product remains almost constant until 50 K, and then increases until reaching a maximum value of 26.75 cm^3 K mol^{-1} at 8 K. Below this temperature, the $\chi_M T$ value decreases down to 2 K to reach a value of 20.48 cm^3 K mol^{-1} (Figure 4). The increase in the $\chi_M T$ product from 50 to 8 K is due to the ferromagnetic Ni^{II}-Gd^{III} interaction transmitted by the diphenoxido bridging groups, whereas the decrease below 8 K is due to the Ni^{II}-Ni^{II} antiferromagnetic interaction mediated by the naphthelenediimine bridges and the zero field splitting of the Ni^{II} ions.

The magnetic properties of **3** have been evaluated employing the Hamiltonian given in equation 1, assuming that all the metal ions have the same g value and the same D value for the two Ni^{II} ions. The best simultaneous fit of the susceptibility and

magnetization data for **3** leads to the following parameters: $J = +2.3$ cm^{-1}, $J_I = -1.0$ cm^{-1}, $g = 2.2$ and $|D| = 6.2$ cm^{-1} with R = 2×10^{-5}. The extracted D value is, as expected, similar to that observed for complex **1**. When D is fixed to zero, the best fit leads to the following magnetic parameters: $J = +2.3$ cm^{-1}, $J_1 = -1.1$ cm^{-1} and $g = 2.2$ with R = 4×10^{-5}. As in the case of complex **1**, the J and g values remain essentially constant, whereas J_I becomes slightly larger. This fact clearly indicates that D and J_I are correlated, so that the extracted J_1 value from the latter fitting procedure can be considered as the higher limit of this parameter. It is worth mentioning that, at variance with **1**, the field dependence of the magnetization for **3** (Figure 4) does not show a clear sigmoidal shape at low field, which is due to the weak Ni^{II}-Ni^{II} antiferromagnetic interaction observed for the latter.

In order to obtain an estimate of the zero field splitting parameter (D) and to confirm the nature of the magnetic exchange interaction transmitted by the naphthalenediimine bridges (J_I) we decided to study the magnetic properties of the isostructural compound **5**. The $\chi_M T$ product at room temperature for **5** (2.67 cm^3 K mol^{-1}) is larger, albeit close to the expected value for two non-coupled Ni^{II} ions (assuming $g_{Ni} = 2.2$; 2.42 cm^3 K mol^{-1}). As the temperature decreases, $\chi_M T$ remains approximately constant until 25 K and then sharply decreases down to 2 K reaching a value of 0.96 cm^3 K mol^{-1} (Figure 4).This behaviour is mainly due to the existence of very weak antiferromagnetic interactions between the Ni^{II} ions transmitted by the naphthelenediimine bridging groups and/or the zero field splitting of Ni^{II} ions. In order to quantitatively analyse the magnetic properties of **5** we have used the following Hamiltonian:

$$\hat{H} = -J_1\left(\hat{S}_{Ni1}\hat{S}_{Ni2}\right) + \sum_{i=1}^{2} D_{Nii}\left(\hat{S}_{zNii}^2 - 2/3\right) + \mu_B H \left[\sum_{i=1}^{2} g_{Nii}\hat{S}_{Nii}\right] \text{ (equation 2)}$$

where the symbols have their usual meanings (Figure 4). The best simultaneous fit of $\chi_M T$ and the field dependence of magnetization with the above Hamiltonian, using the PHI program, led to the following parameters: $J_I = -0.76$ cm^{-1}, $g = 2.21$, $|D| = 7.75$ cm^{-1}, R = 1.0×10^{-5}. The extracted parameters confirm that the magnetic exchange interaction between the Ni^{II} ions is antiferromagnetic in nature and very weak in magnitude. As D and J_1 are correlated, we have obtained the approximate limits for both parameters by fitting the magnetic properties alternatively with either D or J_1 fixed to zero. Thus best fit with $D = 0$, leads to $J_I = -1.4$ cm^{-1}, $g = 2.21$ and R = 6.0×10^{-4}, whereas when J_1 is fixed to zero the extracted parameters are: $g = 2.21$, $|D| =$

15 cm^{-1} and R = 1.0 x10^{-3}. As expected, the quality of the fits is worse and the extracted values can be considered as the limits for J_l and D, respectively. The above results support the sign and magnitude of the magnetic exchange interaction between the Ni^{II} ions, as well as the magnitude of D extracted for **3**.

It is worth noting that the combination of ferromagnetic Ni-Gd interactions and antiferromagnetic Ni-Ni interactions, leads to a $S_T = 0$ ground spin state (Figure 4). Theoretical and experimental magneto-structural correlations [19] (Table 2) have shown that the ferromagnetic exchange interaction between Ni^{II} and Gd^{III} ions in Ni^{II}-Gd^{III} complexes containing diphenoxido-bridging units mainly depends on the Ni-O-Gd bond angle (θ) and the dihedral angle between the O-Ni-O and O-Gd-O planes (β), so that the ferromagnetic interaction enhances as the former angle increases and the latter angle decreases. Indeed, the first angle plays a more important role in determining the magnitude of the ferromagnetic coupling. For complexes **1** and **3**, with mean θ and β angles of 108.64° and 4.4° and 107.89° and 5.0°, respectively, the existing magneto-structural correlations suggest ferromagnetic interactions between +2 and +4 cm^{-1} (Table 2), which agrees well with the experimental results. The fact that the θ and β angles observed in **1** are larger and smaller, respectively, than those found for **3**, could justify the larger J value extracted for the former complex. It is worth mentioning that complex **1** exhibits the largest J value ever found for diphenoxido-bridged Ni^{II} and Gd^{II} complexes.

Table 2: Magneto-structural data for complexes containing dinuclear Ni-Gd units with diphenoxido bridging groups.

Complex	J_{exp}(cm^{-1})	θ (°)[a]	β (°)[a]	Gd$\cdots$Ni (Å)[a]	Ref.
[Ni(H$_2$O)(μ-L^1)Ln(NO$_3$)$_3$]·2CH$_3$OH	+2.16	109.4	2.3	3.565	[19]
[L^{2}Ni(H$_2$O)$_2$Gd(NO$_3$)$_3$]	+3.6	107.2	2.8	3.522	[20]
[Ni(CH$_3$CN)$_2$(valpan)Gd(NO$_3$)$_3$]·CH$_3$CN	+2.3	106.1	0.22	3.467	[21]
[Ni(μ-L^1)(μ-Ac)Gd(NO$_3$)$_2$]	+1.38	104.4	21.4	3.456	[19]
[Ni(valpan)(MeOH)(ac)Gd(hfac)$_2$]	+2.2	102.1	13.5	3.384	[22]

[(H$_2$O)Ni(ovan)$_2$(μ-NO$_3$)Gd(ovan)(NO$_3$)$_2$]H$_2$O	+1.36	101.6	0.8	3.324	[23]
[L^{3}Ni(H$_2$O)(μ-OAc)Gd(NO$_3$)$_2$]·CH$_3$CN	+1.54	103.3	14.8	3.443	[24]
[Ni$_2$Gd$_2$L2(CH$_3$CN)$_3$(NO$_3$)$_6$(H$_2$O)]·(CH$_3$CN)$_2$(H$_2$O)	+4.1	107.87[b] 109.43[b]	3.12[b] 5.77[b]	3.529[b] 3.569[b]	This work
[Ni$_2$Gd$_2$(L1)$_2$(H$_2$O)$_{1.5}$(CH$_3$CN)$_2$(NO$_3$)$_6$]·CH$_3$CN	+1.80	106.8[b] 105.3[b]	1[b] 7.78[b]	3.548[b] 3.465[b]	[9]
[Ni$_2$Gd$_2$(L3)$_2$(CH$_3$CN)$_4$(NO$_3$)$_6$]·(CH$_3$CN)$_4$	+2.30	107.83[b] 107.95[b]	7.40 2.61	3.533[b] 3.538[b]	This work
[Ni(o-van)$_2$(H$_2$O)$_2$Gd(NO$_3$)$_3$]	+2.48	106.5 107.48	2.04	3.512	[25]
[Cl$_2$NiL^{2}Gd(H$_2$O)$_4$]Cl(H$_2$O)$_2$	+3.6	108.51 108.18	1.73	3.520	[26]
[Ni(L^4)Gd(DBM)$_3$]	+2.22	103.70 104.58	22.89	3.429	[27]

[a] average values; [b] values for each NiGd unit in the tetranuclear complex ; H$_2$L^1= N,N',N"-trimethyl-N,N"-bis(2-hydroxi-3-methoxy-5-methylbenzyl)diethylentriamine. H$_2$L^2= N,N'-2,2-dimethylpropylendi(3-methoxysalicylideneiminate. valpan= N,N'-propylendi(3-methoxysalicylideniminate). Ovan= o-vanilline. H$_2$L^3= Schiff base from the 1:2 condensation of 1,1'-diacetylferrozendihydrazone. H$_2$L1= N,N'-Bis(2-hydroxy-3-methoxy-benzyliden)-1,3-diaminobenzene. H$_2$L2= N,N'-Bis(2-hydroxy-3-methoxy-benzyliden)-1,4-diaminobenzene. H$_2$L3 = N,N'-Bis(2-hydroxy-3-methoxy-benzyliden)-1,4-diaminonaphatalene. H$_2$L^4= N,N'-dimethyl-N,N'-(2-hydroxy-3-methoxy-5-methylbenzyl)ethylenediamine. HDMB= 1,3-diphenylpropane-1,3-dione.

As far as we know, no examples of magneto-structural characterized Ni^{II} metallocyclophane complexes containing either 1,4-disubstituted benzene or 1,5-disubstituted naphthalene dinucleating bridging ligands have been reported so far. However, oxamate-based dicopper(II) metallacyclophanes with 1,4-disubstituted benzene or 1,5-disubstituted naphthalene bridging groups and an even number of aromatic carbon atoms between the nitrogen atoms have been shown to exhibit antiferromagnetic interactions, in keeping with a spin polarization mechanism [1j]. Moreover, experimental and theoretical studies have shown that magnetic coupling through the π-type orbital pathways not only decrease with intermetallic distance (due to the increasing number of repetitive units in the bridging spacer) but also on going from α,α′-to β,β′-substitution [1j]. In view of the above considerations, for compounds **1** and **3**, which both have an even number of aromatic carbon atoms between the nitrogen atoms, one can predict antiferromagnetic interactions between the Ni^{II} ions, which agrees with the experimental results. In addition, the fact that the

antiferromagnetic interaction for **1** is stronger than for **3** can be justified by the longer intermetallic Ni···Ni distance and the α,α′-substitution for the latter.

In order to support the magnitude and nature of the experimental magnetic exchange interactions between the Ni^{II} and Gd^{III} ions transmitted by the diphenoxido bridging groups (described by J_{NiGd}), and the Ni-Ni coupling through the 1,4-phenylenediimine or 1,5 naphthalenediimine bridging fragments (J_{NiNi}), we have carried out DFT theoretical calculations based on the X-ray crystal structures of **1** and **3**. These calculations were performed using the SIESTA (Spanish Initiative for Electronic Simulations with Thousands of Atoms) code [28] together with the PBE functional [29]. Only valence electrons are included in the calculations, with the core being replaced by norm-conserving scalar relativistic pseudopotentials factorized in the Kleinman-Bylander form [30]. The pseudopotentials are generated according to the procedure of Trouiller and Martins [31]. For gadolinium atoms, we used the pseudopotential and triple-ζ basis set proposed by Pollet et al. [32]. We have also employed a numerical basis set of triple-ζ quality functions for the nickel atoms and a double-ζ one with polarization functions for the main group elements. The broken symmetry approximation (without spin-projection) has been employed [33-35].

The calculated J_{NiGd} values are +4.5 cm^{-1} and +4.8 cm^{-1} for **1** (both halves of the molecule are structurally and magnetically different) and +3.05 cm^{-1} for **3**, while J_{NiNi} is -7 cm^{-1} for **1** and -0.87 cm^{-1} for **3** (the magnetic coupling has been considered equal for the two molecules in the unit cell). These values agree in sign and are close in magnitude to those extracted from magnetic measurements, and confirm that the antiferromagnetic interaction between the Ni^{II} ions is weaker for **3** than for **1**. It should be noted that the elimination of the Gd^{III} ions in the X-ray structure of **1** leads to a significant lower J_{NiNi} value of -4.2 cm^{-1}. It is worth highlighting that the differences observed between the experimental and calculated magnetic exchange coupling constants are mainly due to the inherent limitations of the calculation method. DFT calculations also confirm that the magnetic coupling between the Ni^{II} ions through the π-extended system is due to a spin polarisation mechanism, because of the topological alternation of the spin densities at the adjacent carbon atoms of the acene linker, which results from dynamic spin polarization (see Tables 3 and 4 and Figure 5). As expected, the alternating spin density in the acene rings is higher for complex **1** than for **3**.

*Table 3: Spin densities (in e$^-$) for selected atoms of **1**.*

Atoms	Spin densities	Atoms	Spin densities
Ni1	+1.766	$N_{eq\text{-}Ni2}$[a][b]	−0.047
Gd1	+7.068	$N_{ax\text{-}Ni1}$[a][c]	+0.037
Ni2	−1.761	$N/O_{ax\text{-}Ni2}$[a][c][d]	−0.035
Gd2	−7.063	$O_{methoxy\text{-}Gd1}$[a]	−0.005
$O_{bridge\text{-}Ni1Gd1}$[a]	+0.035	$O_{methoxy\text{-}Gd2}$[a]	+0.004
$O_{bridge\text{-}Ni2Gd2}$[a]	−0.034	$O_{nitrates\text{-}Gd1}$[a][e]	−0.009
$N_{eq\text{-}Ni1}$[a][b]	+0.063	$O_{nitrates\text{-}Gd2}$[a][e]	+0.007

[a]*Average values;* [b]*Equatorial nitrogen atoms in the Ni^{II} coordination sphere;* [c]*Axial nitrogen atoms belonging to solvent molecules;* [d]*Average value of the oxygen and nitrogen atoms with similar spin densities (-0.040 y -0.030, respectively);* [e]*Spin densities values for five and six nitrate oxygen atoms linked to Gd1 and Gd2, respectively.*

*Table 4: Spin densities (in e-) for selected atoms of **3**.*

Atoms	Spin densities	Atoms	Spin densities
Ni1	+1.773	Gd1	+7.059
Ni2	−1.773	Gd2	−7.058
PATHWAY A[a],[d]			
Ni1	+1.773	C10	−0.009
N1	+0.049	C6	+0.006
C1	−0.006	N2	−0.044
C2	+0.008	Ni2	−1.773
PATHWAY B[b],[d]			
Ni1	+1.773	C4	+0.008
N1	+0.049	C5	−0.004
C1	−0.006	C6	+0.006
C2	+0.008	N2	−0.044

C3	−0.004	Ni2	−1.773
PATHWAY C[c,d]			
Ni1	+1.773	C9	+0.003
N1	+0.049	C10	−0.009
C1	−0.006	C6	+0.006
C7	+0.004	N2	−0.044
C8	−0.007	Ni2	−1.773

[a]*inside naphthalene;* [b]*clockwise;* [c]*counterclockwise;* [d]*values obtained for the naphthalene upper ring as the lower one present similar values.*
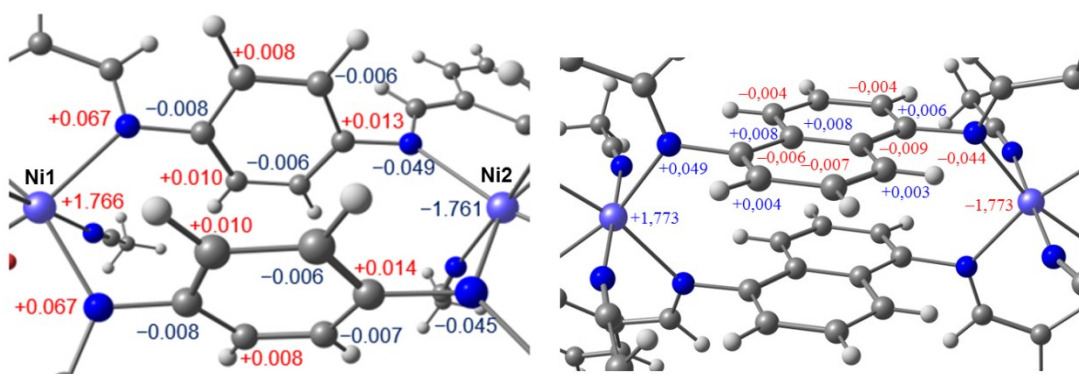

*Figure 5.- Selected spin densities for complexes **1** (left) and **3** (right). Alternating spin densities in the acene rings highlight the spin polarization mechanism.*

At room temperature, the $\chi_M T$ value for **2** (32.07 cm^3 K mol^{-1}) is higher, but compatible, with the expected value for two isolated Ni^{II} ions ($S = 1$; $g_{Ni} = 2.0$) and two isolated Dy^{III} ions in the free ion approximation ($^6H_{15/2}$, $g_{Gd} = 4/3$) of 30.34 cm^3 K mol^{-1}. By lowering the temperature from 300 K to 10 K, the $\chi_M T$ product decreases slowly from 32.07 cm^3 K mol^{-1} to 28.52 cm^3 K mol^{-1}. Below 10 K, the $\chi_M T$ product decreases drastically to reach a value of 9.02 cm^3 K mol^{-1} at 2 K (Figure 6).
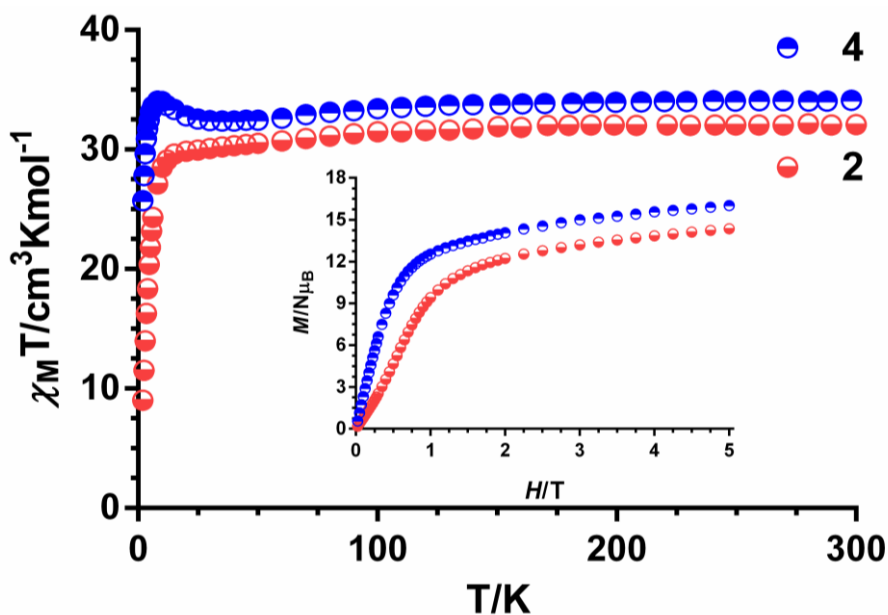
*Figure 6.-Temperature dependence of $\chi_M T$ product for complexes **2** and **4**. Field dependence of the magnetization at 2 K (inset).*

The slight decrease of the $\chi_M T$ product between 300 K and 10 K is due to the depopulation of the M_J sublevels of the Dy^{III} ion, which arise from the ligand-field splitting of the corresponding spin-orbit coupling levels. Moreover, the sharp decrease of the $\chi_M T$ product below 10 K is mainly due to combined effects of the Ni-Ni antiferromagnetic interaction, zero field splitting of the Ni^{II} ions, and the anisotropy of the Dy^{III} ions. The fact that this compound does not show an increase in the $\chi_M T$ product at low temperature could be due to: (i) the antiferromagnetic nature of the Ni-Ni interaction, and/or (ii) the Ni-Dy interaction being ferromagnetic. However, the combined effects of the antiferromagnetic Ni-Ni interaction, zero field splitting of the Ni^{II} ions, and the anisotropy of the Dy^{III} ions (all of which would produce a decrease in $\chi_M T$ at low temperature) overcome the expected increase of $\chi_M T$ at low temperature. As for (i), it is worth noting that previous studies on isostructural Ni^{II}-Ln^{III} complexes have shown that Gd^{III}, Tb^{III} and Dy^{III} compounds generally display magnetic exchange interactions of the same nature (usually ferromagnetic) [36]. Therefore, it is reasonable to assume that Ln^{III} and Ni^{II} are ferromagnetically coupled.

The field dependence of the magnetization at 2 K for **2** (Figure 6, inset) shows a relatively slow and sigmoidal increase of the magnetization at low fields, followed by a linear increase without clear saturation above 2 T. The sigmoidal shape of the magnetization

curve at low fields, as in the case of complex **1**, is due to the Ni^{II}-Ni^{II} antiferromagnetic interaction. The fact that saturation cannot be reached at the maximum applied field of 5 T, could be due to the existence of a large magnetic anisotropy and/or to the presence of energy levels very close to the ground energy level which can be magnetically and thermally populated. The magnetization under the highest applied field of 5 T is 14.34 $N\mu_B$, close to that expected for two non-interacting Dy^{III} ions with significant magnetic anisotropy arising from crystal-field effects ($M \sim 5~N\mu_B$ for each Dy^{III} ion) [37] and two Ni^{II} ions ($M \sim 2~N\mu_B$ for each Ni^{II} ion).

At room temperature the $\chi_M T$ product of complex **4** (34.11 cm^3 K mol^{-1}) is somewhat larger than the expected for two Dy^{III} ($^6H_{15/2}$, g_{Dy} = 4/3) and two Ni^{II} (S = 1; g_{Ni} = 2.0) magnetically isolated ions (30.72 cm^3 K mol^{-1}). As the temperature decreases from room temperature, the $\chi_M T$ product first decreases to reach a minimum at around 35 K (32.37 cm^3 K mol^{-1}), before increasing to a maximum of 34.06 cm^3 K mol^{-1} at 8 K. Below this temperature, the $\chi_M T$ value sharply decreases down to 2 K, reaching a value of 25.72 cm^3 K mol^{-1} (Figure 6). The slow decrease of $\chi_M T$ from 300 K to 35 K, as usual, is due to the depopulation of the M_J sublevels of the Dy^{III} ion, which arise from the splitting of the spin-orbit coupling levels caused by ligand field effects. The small increase of $\chi_M T$ between 35 and 8 K, is due to the ferromagnetic Ni-Dy interaction, while the sharp decrease below 8 K is due to the antiferromagnetic Ni-Ni interaction and zero field splitting of the Ni^{II} ions. In this case, the ferromagnetic Ni^{II}-Dy^{III} interaction is strong enough to overcome the effect of the depopulation of the M_J sublevels and therefore an increase in $\chi_M T$ appears at low temperature.

The field dependence of the magnetization for **4** (Figure 6, inset) shows a fast increase in the magnetization with field until 2 T, and then a slow linear increase without reaching saturation at the maximum applied field of 5 T. This behavior can be due, as in the case of **2**, to the existence of energy levels very close to ground energy level, which can be magnetically and thermally populated, and/or to a large magnetic anisotropy. The value at 5 T (20.07 $N\mu_B$) is lower than that expected for two Dy^{III} ions ferromagnetically coupled to two Ni^{II} ions (24 $N\mu_B$). As indicated elsewhere, this fact is due to crystal field splitting of the Dy^{III} ions ground multiplet (J = 15/2), which leads to saturation magnetization values of approximately 5-7 $N\mu_B$ for mononuclear Dy complexes with an axial ground state [37].

Dynamic magnetic measurements of Ni$_2$Ln$_2$ (Ln^{III} = Gd, Dy)

In order to know if complexes **2** and **4** exhibit slow relaxation of the magnetization and SMM behaviour, temperature and frequency dependent dynamic *ac* magnetic susceptibility measurements were carried out in the 2-10 K and 1-1400 Hz ranges, respectively. Dynamic *ac* measurements at zero static magnetic field for complexes **2** and **4** show a strong frequency dependence of the out-of-phase component, $\chi"_M$, below 5 K, but without reaching a maximum above 2 K. This behaviour could be due to either: (i) the magnetization cannot be trapped above 2 K because the anisotropy barrier for magnetization reversal is a too small, or (ii) the existence of a very fast resonant zero-field QTM. When the ac measurements were carried out in the presence of a small external field of 0.1 T to fully or partly suppress QTM, the same results as at zero field were obtained (Figure 7). This fact seems to indicate that the absence of maxima in the out-of-phase ac susceptibility measurements below 2 K is due to (i) rather than to (ii). The small effective energy barrier for magnetization reversal in **2** and **4** can be justified by the small J_{NiDy} value expected for these complexes (J_{NiGd} values of +4.1 cm^{-1} and +2.3 cm^{-1} have been observed for the isostructural NiGd complexes **1** and **3**, respectively). This is because the weak Ni-Dy magnetic coupling leads to a small separation between the low-lying split energy sublevels, which favour mixing of low-lying excited states into the ground state and then QTM. This ultimately leads to a small effective energy barrier for magnetization reversal. As the *ac* data for **2** and **4** could not be fitted to the Debye model (no peaks are observed in the studied frequency range, Figure 7), we have used an alternative approach to extract the relaxation parameters from the *ac* data. This approach is based on the fact that the ratio between the out-of-phase and in phase *ac* susceptibility can be expressed in an approximate manner as $\chi"_M/\chi'_M = 2\pi f \tau$. The replacement in this equation of the relaxation time (τ) by its expression for each relaxation mechanism would allow the extraction of the corresponding relaxation parameters. If we assume that the relaxation takes place exclusively through an Orbach relaxation mechanism, for which $\tau = \tau_o \exp(-U_{eff}/k_B T)$, the following equation can be obtained:

$$ln(\chi''_M|\chi'_M) = ln(2\pi f \tau_0) - U_{eff}/k_B T \quad \text{(equation 3)}$$

The energy barrier can be approximately estimated by fitting the experimental χ''/χ' data to the above equation (Figure 7). The best fit at different frequencies led to the following

parameters: $U_{eff}/k_B \approx 19$ K and $\tau_0 \approx 1.6 \times 10^{-8}$ s and $U_{eff}/k_B \approx 15.9$ K and $\tau_0 \approx 2.6 \times 10^{-7}$ s, for **2** and **4**, respectively.

The extracted parameters are similar but slightly larger than those found in similar diphenoxide-bridged Ni^{II}-Gd^{III} complexes showing slow relaxation at zero-field [19], including the analogous Dy-Ni-Ni-Dy complex (**2a**) with the Schiff base ligand, N, N'-bis(3-methoxysalicylidene)-1,3-diaminobenzene [9]. The fact that the U_{eff} value for this complex of 11.6 K (using the same method for extracting U_{eff} as for **2** and **4**, Figure S1) is lower than that of **4** which is, in turn, lower than that of complex **2**, can be justified by the inverse order observed for their respective J_{NiGd} coupling constants: +1.80 (**2a** in ref 9) < +2.30 (**3**) < +4.1 (**1**). This is because, as the Ni-Dy magnetic coupling constants become weaker, QTM is favoured, leading to lower values of U_{eff}.
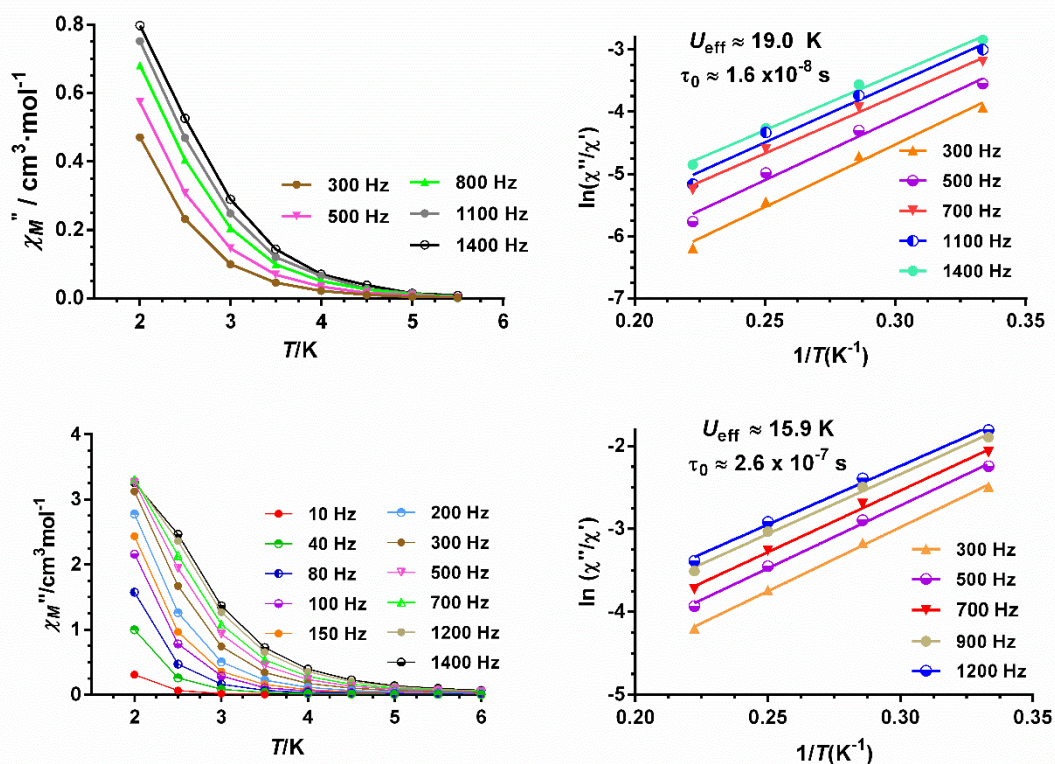

Figure 7.- Temperature dependence of the out-of-phase signals for **2** (top left) and **4** (bottom left). Solid lines are a guide for the eye. Temperature dependence of the ratio of the imaginary and real components of the *ac* susceptibility at the indicated frequencies and at zero-field for **2** (top right) and **4** (bottom right). Solid lines with corresponding colour represent the best fit of the experimental data to equation 3.

Dc susceptibility and magnetization studies of Co₂Ln₂ (Lnᴵᴵᴵ = Gd, Dy)

The magnetic properties for **6** and **7** in the form of $\chi_M T$ *vs* T (χ_M is the molar magnetic susceptibility per $Co^{II}_2Ln^{III}_2$ unit) are displayed in Figure 8.
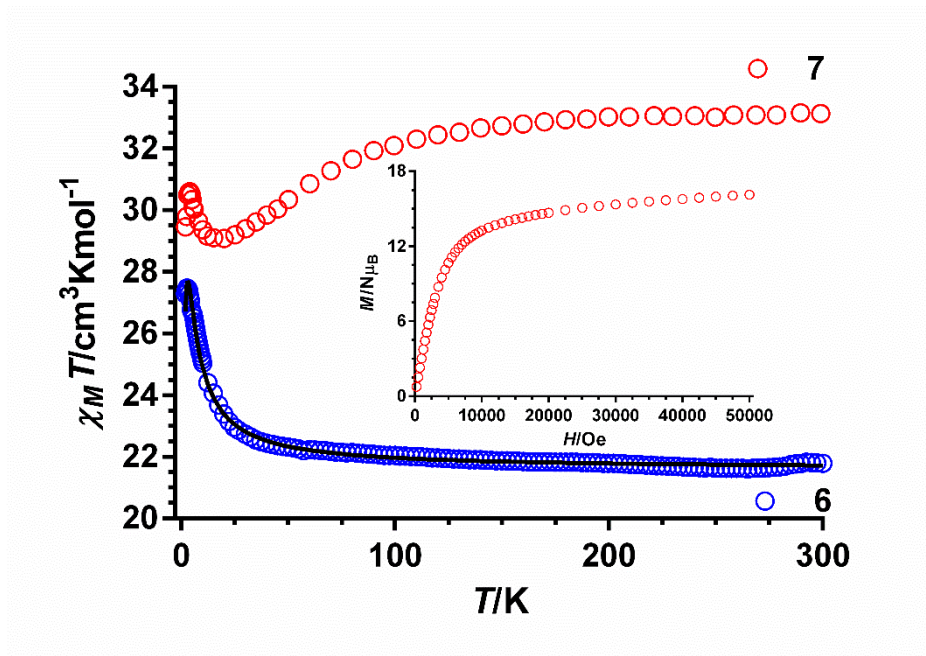

Figure 8.- Temperature dependence of $\chi_M T$ for complexes **6** and **7**. Field dependence of **7** at 2 K (inset).

At room temperature, the $\chi_M T$ value for **6** (21.79 cm³ K mol⁻¹) is larger than that expected for non-interacting Co^{II} ($S = 3/2$) and Gd^{III} ($S = 7/2$) ions (19.63cm³ mol⁻¹ K with $g = 2$), which may be due to both the orbital contribution of the octahedral Co^{II} ion with a $^4T_{1g}$ ground term, and the ferromagnetic interaction between Co^{II} and Gd^{III} ions (see below). On lowering the temperature, the $\chi_M T$ value for **6** first slowly increases from room temperature until approximately 25 K and then shows an abrupt increase to a value of 27.47 cm³ K mol⁻¹ at 3 K. Below this temperature, the $\chi_M T$ product slightly decreases down to 1.9 K to reach a value of 27.28 cm³ K mol⁻¹. This behaviour suggests the existence of a ferromagnetic interaction between Co^{II} and Gd^{III} ions and probably very weak antiferromagnetic coupling between Co^{II} ions. It is well known that the Co^{II} orbital contribution is significantly quenched when the Co^{II} coordination sphere deviates from the ideal octahedral geometry [38]. In such cases there is no appreciable decrease of the $\chi_M T$ in the high temperature region (which is due to the spin-orbit coupling effects) and the Co^{II} ion approximately follows the Curie law. In agreement with this, compound **6**,

having a significantly distorted coordination sphere, shows a steady increase in $\chi_M T$ from room temperature. In view of these considerations, and for the sake of simplicity, the magnetic susceptibility data of compound **6** were analysed using an isotropic Hamiltonian. We emphasise that the magnetic parameters derived from this Hamiltonian can only be viewed as an approximation.

The magnetic properties of **6** have been analysed using the following Hamiltonian:

$$H = -J(S_{Co1}S_{Gd1} + S_{Co2}S_{Gd2}) - J_1(S_{Co1}S_{Co2}) \quad \text{(equation 4)}$$

where J and J_1 are the magnetic exchange coupling constants between the Co^{II} and Gd^{III} ions through the diphenoxido bridging ligands, and between the Co^{II} ions through the naphthalenediimine bridging groups, respectively. From the best fit of the magnetic data, the following parameters have been extracted: $J = +0.62$ cm^{-1}, $J_1 = -0.26$ cm^{-1}, $g = 2.10$ and R = 7×10^{-5}. We unfortunately failed to make the isostructural Co_2Y_2 complex in order to evaluate the magnetic interaction between the Co^{II} ions directly.

If we assume the same magneto-structural correlation for the Co^{II}-Gd^{III} complexes as for the Ni^{II}-Gd^{III} complexes with diphenoxido bridging ligands, the ferromagnetic interaction would mainly depend on the Co-O-Gd angles (θ) and the planarity of the Co^{II}-(O)$_2$-Gd^{III} described by the dihedral angle (β) between the O-Co-O and O-Gd-O planes in the bridging fragment. Thus, the ferromagnetic exchange interaction would increase with increasing θ and decreasing β. In fact, the experimental values of J for other dinuclear Co^{II}-Gd^{III} complexes with diphenoxide bridging ligands agree with those predicted from these magneto-structural correlations. Thus, for θ and β in the ranges 108°-112° and 3.7°-4.2°, respectively, the J values between +0.7 and +0.9 cm^{-1} are found [22,38b,39]. For **6**, with an almost planar Co^{II}-(O)$_2$-Gd^{III} fragment ($\beta \sim 3.6$) and with θ angles of ~108 °, the observed J value of +0.6 cm^{-1} is not unexpected. Moreover, the fact that the Co^{II} coordination sphere of **6** is significantly distorted could explain the relatively low value of J. Nevertheless, deviations from these structural correlations can be mainly attributed to the diversity of bridging (and terminal) ligands present in these species [22, 38b,39].

The nature of the magnetic interaction between Co^{II} ions in complexes containing 1,5-naphthalenediimine bridges has not yet been studied. However, if it assumed, as for the Ni^{II} counterparts, that the intramolecular interactions through 1,5 naphthalenediimine bridges take place by a spin polarization mechanism, an antiferromagnetic interaction

between the Co^{II} ions can be predicted for an even number of atoms between metal centres, which matches well with experimental results. The fact that the J value for **6** is much lower than that observed for the $Ni^{II}_2Gd^{III}_2$ counterpart **3** could be due to the presence of more magnetic orbitals in Co^{II} and/or to the different arrangement of the 1,5-naphthalenediimine bridges. In this regard, the naphthyl rings of the two ligand strands in **3** are parallel and coincident whereas in **6** they are approximately parallel, giving rise to a non-eclipsed disposition. That is, the ligand arrangement in **6** gives rise to a significant distortion of the Co^{II} coordination sphere, which in turn could lead to poorer overlap between the Co^{II} magnetic orbitals and the π system than in the case of **3**.

Despite the ferromagnetic Co^{II}-Gd^{III} interaction, the field dependence of the magnetization at 2 K for complex **6** (Figure 9) shows a relatively slow increase in the magnetization at low field until 2 T (likely due to the weak antiferromagnetic interaction between the Co^{II}) ions), followed by a linear increase to the maximum applied field of 5 T. The lack of saturation is due to the existence of a large magnetic anisotropy and /or energy levels very close to the ground energy level which can be magnetically and thermally populated. Nevertheless, the magnetisation value of 21.2 $N\mu_B$ at 5 T is close to that expected for two pairs of ferromagnetic coupled Co^{II} and Gd^{III} ions (with S_{Co} = 3/2, S_{Gd} = 7/2 and g = 2.0 for both ions).

The $\chi_M T$ product for **7** at room temperature (33.12 cm^3 K mol^{-1}) is close to that expected (32.08 cm^3 K mol^{-1}) for independent Co^{II} (S = 3/2 with g_{Co} = 2.0) and Dy^{III} (4f^9, J = 15/2, S = 5/2, L = 5, $^6H_{15/2}$, g_J = 4/3) ions in the free-ion approximation. The $\chi_M T$ value decreases with decreasing temperature down to a minimum value of 29.1 cm^3 K mol^{-1} at 20 K, then increases at lower temperatures, reaching a maximum value of 30.6 cm^3 K mol^{-1} at 4 K. Below this temperature, $\chi_M T$ decreases down to 2 K to reach a value of 29.45 cm^3 K mol^{-1}. The decrease between 300 and 20 K is due to the thermal depopulation of the M_J sublevels of the Dy^{III} ions and to the depopulation of the spin-orbit coupling levels of the Co^{II} ion. The increase of $\chi_M T$ value is due to the ferromagnetic interactions between Co^{II} and Dy^{III} ions, while the decrease from 4 K is due to the weak antiferromagnetic interactions between Co^{II} ions.

The *M vs H* curve for **7** (Figure 8) displays a rapid increase in the magnetization at low fields, followed by a linear increase without reaching saturation to 5 T. The linear variation of the magnetization at high fields suggests the presence of magnetic anisotropy

and/or partially populated excited states. It is worth noting that the magnetization value at 5 T (19.91 $N\mu_B$) is much lower than the expected saturation value for two Dy^{III} ions ferromagnetically coupled to two Co^{II} ions with $S = 3/2$ (26 $N\mu_B$), which is again due to the ground multiplet splitting of the Dy^{III} ion ($J = 15/2$) promoted by ligand field effects [37].

Compound **7** does not show out-of-phase ac susceptibility signals above 2 K under zero or applied magnetic fields, which indicates the absence of slow relaxation of the magnetization and SMM behaviour for this complex. This behaviour highlights once again that the introduction of two anisotropic ions such as Co^{II} and Ln^{III} does not guarantee a larger uniaxial anisotropy, as the local anisotropies can be destructive. This, together with the very weak J_{CoDy} expected for this compound could lead to U_{eff} values so small that slow relaxation can not be observed about 2 K.

Magnetocaloric effects of the M_2Gd_2 complexes (M^{II} = Ni, Co)

The magnetic entropy changes ($-\Delta S_m$) that characterize the magnetocaloric properties of **1, 3** and **6** can be calculated from the experimental isothermal field dependent magnetization data (Figures 9 and 10) by making use of the Maxwell relation:

$$\Delta S_M = (T, \Delta B) = \int_{B_i}^{B_f} \left[\frac{\partial M(T,B)}{dT} \right]_B dB \qquad \text{(equation 5)}$$

where B_i and B_f are the initial and final applied magnetic fields. The values of $-\Delta S_m$ (Figure 9) for **1** increase as the temperature decreases from 6 to 3 K until 3 T, but at higher fields the largest values occur at 4 K. However, for **3** and **6**, the $-\Delta S_m$ values under any field increase as the temperature decreases from 6 to 3 K. This can be due to the strong Ni-Ni magnetic interaction observed in **1** compared to those found for complexes **3** and **6**. The maximum values of $-\Delta S_m$ are achieved at an applied field change $\Delta B = 5$ T and are as follows: 14.5 J kg^{-1} K^{-1} at $T = 4$ K (for **1**), 17.5 J kg^{-1} K^{-1} (for **3**) and 15.9 J kg^{-1} K^{-1} (for **6**). It should be noted that despite the antiferromagnetic M-M interaction these compounds exhibit relatively large changes in $-\Delta S_m$, consistent with easy spin polarization under small magnetic fields. As expected for the existence of non-magnetic organic groups in these complexes, the extracted $-\Delta S_m$ values are lower than those calculated for the whole magnetic entropy per mole $2R\ln(2S_M + 1) + 2R\ln(2S_M + 1)$, of 6.36R for

complexes **1** and **3** ($-\Delta S_m$ values of 29.50 J kg^{-1} K^{-1} and 26.67 J kg^{-1} K^{-1}) and 6.93 R ($-\Delta S_m$ = 26.14 J kg^{-1} K-1) for complex **6**. The $-\Delta S_m$ value for **1** is rather lower than that of **3**, which can be justified by the larger values of J and J_1 found for the former. This is also the reason why compound **1a** (the analogous Gd-Ni-Ni-Gd complex with the Schiff base ligand, N, N$^{'}$-bis(3-methoxysalicylidene)-1,3-diaminobenzene), with J and J_1 weaker than those of **1** and **3** exhibits a larger MCE (18.53 J kg^{-1} K^{-1}). Moreover, in the case of **1a** the ferromagnetic interactions between the Ni^{II} ions leads to a high spin ground state ($S = 9$), which also favours a larger $-\Delta S_m$ value. In the case of compound **6**, with weaker J and J_1, the $-\Delta S_m$ value should be even larger than that of **1a**. However, the extracted $-\Delta S_m$ for **6** is smaller than those for **1a** and **3**. This fact can be justified by the presence of the anisotropic Co^{II} ion in **6**, which is known to decrease the MCE [11].
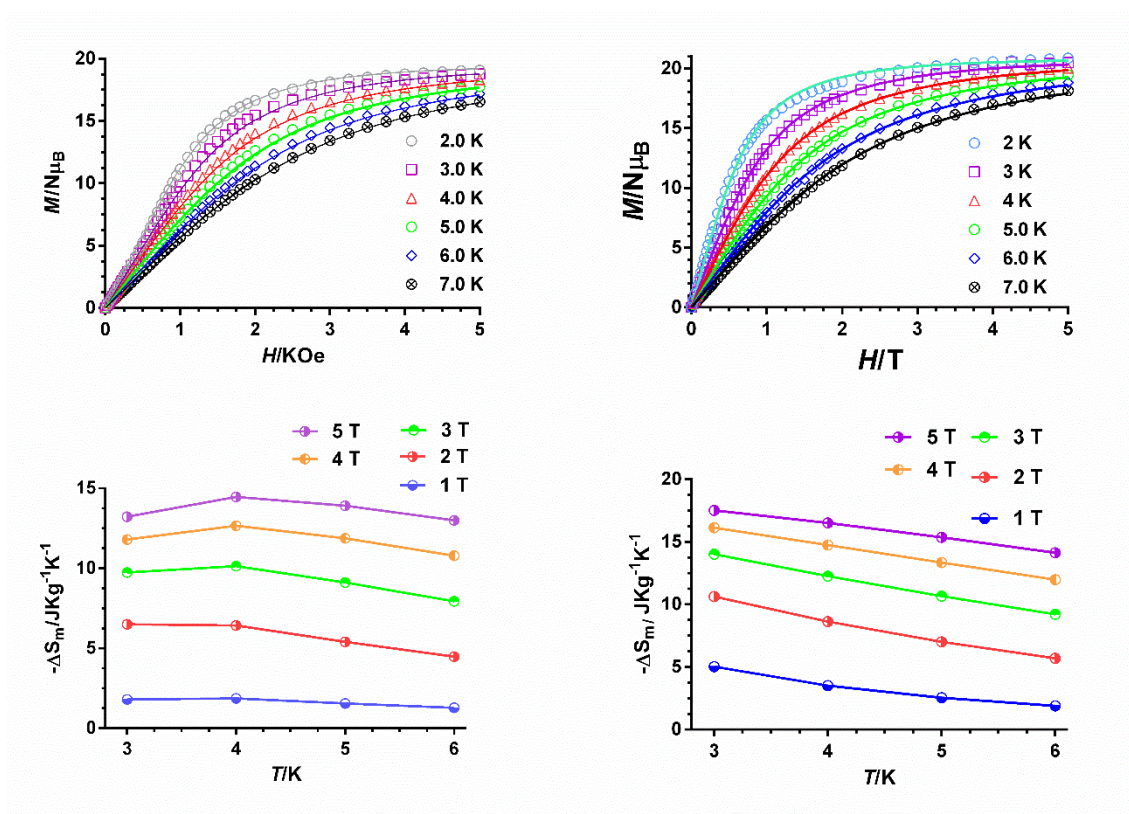

*Figure 9: (Top) Field dependence of the magnetisation for **1** (left) and **3** (right) in the 2-7 K temperature range. (Bottom) Magnetic entropy changes (-ΔS_m) calculated using the magnetization data for **1** (left) and **3** (right).*

It is worth noting that the presence of the antiferromagnetic interactions between the M^{II} ions (M = Ni, Co) in **1**, **3** and **6** leads to MCE lower than that observed for other M-Gd complexes with ferromagnetic coupling and/or large metal ion/ligand ratio [11].
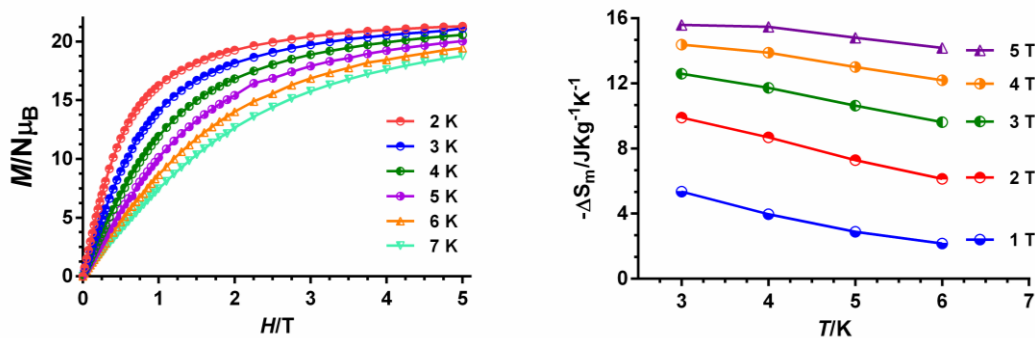

*Figure 10.- Field dependence of the magnetisation for **6** in the 2-7 K temperature range (left). Magnetic entropy changes (-ΔS_m) calculated using the magnetization data for **6** (right).*

Conclusions

The ongoing results demonstrate that tetranuclear linear Ln^{III}-M^{II}-M^{II}-Ln^{III} complexes (M^{II}= Ni, Co; Ln^{III}= Gd, Dy, Y) can be successfully prepared by following the strategy of assembling linear Schiff base ligands, that contain two NOO' tridentate bridging coordination domains well separated by 1,4-phenyl and 1,5-naphtyl spacers, successively with transition metal and lanthanide ions. The NO donor part of each NOO' coordination domain is joined to the transition metal ion, whereas the OO' counterpart is bonded to the lanthanide ion. Therefore, either phenylendiimine or naphthylendiimine bridging groups connect the M^{II} ions, giving rise to 14- and 18-membered M_2 metallacycles, respectively. Moreover, the two-phenoxide groups coordinated to the M^{II} ions at both sides of these metallacycles bridge the M^{II} and Ln^{III} ions, leading ultimately to the M_2Ln_2 molecules. Static *dc* magnetic susceptibility studies reveal the presence of ferromagnetic interactions between M^{II} and Ln^{III} ions through the diphenoxide bridging groups and antiferromagnetic interactions between the M^{II} ions through the 1,4-phenylenediimine or 1,5-naphthalenediimine bridging groups. The even number of aromatic carbon atoms between the nitrogen atoms of these acene-bridging groups, points to a spin polarization mechanism operating for the magnetic interaction between the M^{II} ions. In keeping with this, the fact that

complexes containing the 1,4-phenylenediimine bridging group have stronger antiferromagnetic interactions than those containing 1,5-naphthalenediimine counterparts can be justified by the longer intermetallic $M^{II} \cdots M^{II}$ distances and α,α'-substitution for the latter. The ferromagnetic interactions between M^{II} and Ln^{III} ions are not unexpected in view of the structural features of the $M^{II}(O)_2Ln^{III}$ bridging fragment. DFT calculations confirm the sign and magnitude of the magnetic interactions, as well as spin polarisation mechanism for the magnetic interaction between M^{II} ions. The Ni_2Dy_2 complexes exhibit slow relaxation of the magnetization, albeit without displaying maxima in out-of-phase ac susceptibility measurements below 5 K, whereas the Co_2Dy_2 counterpart does not any SMM behaviour. This difference is likely due to the destructive combination of the local anisotropies of the Co^{II} and Dy^{III} ions and/or to the presumably very weak J_{CoDy} interaction expected for this compound. The extracted U_{eff}/k_B values for the Ni_2Dy_2 complexes and the analogous complex containing the 1,3- phenylenediimine spacer (with an odd number of carbon atoms between the N atoms and a ferromagnetic interaction between the Ni^{II} ions) follows the same order as the magnetic exchange coupling constants. This is because the weaker Ni-Dy magnetic coupling constants favour the mixing of low-lying excited states into the ground state, consequently inducing QTM and lower values of U_{eff}. Changes in magnetocaloric effect between complexes **1**, **3** and **6** follow the expected trend depending upon the nature and magnitude of the exchange interaction and the difference in anisotropy between octahedral Ni^{II} and Co^{II}.

This paper is a tribute to Professor Miguel Julve, one of the most prestigious and renowned researchers in Molecular Magnetism based on Coordination Complexes, on the occasion of his 65th anniversary. He has achieved key milestones in this field over the last forty years and, consequently, has contributed in a decisive manner to its development, evolution and growth. Professor Julve is like a magician, who subtly playing with the tools offered by the Coordination Chemistry has been able to deliberately design and prepare new molecular materials with aesthetically structures and fascinating magnetic properties. Moreover, Professor Julve and his group, at the University of Valencia, has always helped many of us to walk along the exciting and attractive road of Molecular Magnetism. Thanks you very much for your friendship and for your support.

Appendix A. Supplementary data

References

[1] Some reviews: (a) R. Chakrabarty, P. S. Mukherjee, P. J. Stang, Chem. Rev. 111 (2011) 6810– 6918.
(b) T. R. Cook, P. J. Stang, Chem. Rev. 115 (2015) 7001-7045.
(c) A. J. McConnell, C.S. Wood, P.P. Neelakandan, J. R. Nitschke, Chem. Rev. 115 (2015) 7729-7793.
(d) G. R. Newkome, C. N. Moorefield, Chem. Soc. Rev. 44 (2015) 3954-3967.
(e) M. Han, D. M. Engelhard, G. H. Clever, Chem. Soc. Rev. 43 (2014) 1848-1860.
(f) M. L. Saha, S. Neogi, M. Schmittel, Dalton Trans. 43 (2014) 3815-3834.
(g) M. Yoshizawa, J. K. Klosterman, Chem. Soc. Rev. 43 (2014) 1885-1898.
(h) K. Harris, D. Fujita, M. Fujita, Chem. Comm. 49 (2013) 6703-6712.
(i) T. R. Cook, Y. R. Zheng, P. J. Stang,, Chem. Rev. 113 (2013) 734−777.
(j) M. Castellano, R. Ruiz-García, J. Cano, J. Ferrando-Soria, E. Pardo, F. R. Fortea-Perez, S.-E. Stiriba, M. Julve, Francesc Lloret, Acc. Chem. Res. 48 (2015) 510−520.

[2] Some reviews: (a) C. J. Brown, F. D. Toste, R. G. Bergman, K. N. Raymond. Chem. Rev. 115 (2015) 3012– 3035.
(b) M. Lal Saha, X. Yan, P. J. Stang, Acc. Chem. Res. 49 (2016) 2527-2539.
(c) A. J. McConnell, C. S. Wood, P. P. Neelakandan, J. R. Nitschke, Chem. Rev. 115 (2015) 7729– 7793.
(d) M. L. Saha, S. Neogi, M. Schmittel, Dalton Trans. 43 (2014) 3815– 3834.
(e) L. Xu, Y. X. Wang, H. B. Yang, Dalton Trans. 44 (2015) 867– 890.
(f)) H. Amouri, C. Desmarets, J. Moussa, Chem. Rev. 112 (2012) 2015-2041.
(g) S. J. Lee, J. T. Hupp, Coord. Chem. Rev. 250 (2006) 1710-1723.
(h) M. D. Pluth, R. G. Bergman, K. N. Raymond, Acc. Chem. Res. 42 (2009) 1650-1659.

(i) M. Yoshizawa, J. K. Klosterman, M. Fujita, Angew. Chem. Int. Ed. 48 (2009), 3418-34138.

[3] (a) A. J. Hutchings, F. Habib, R. J. Holmberg, I. Korobkov M. Murugesu, Inorg. Chem. 53 (2014) 2102–2112.
(b) H. Li, P. Chen W. Sun L. Zhang P. Yan. Dalton Trans. 45 (2016) 3175-3181.
(c) S.-Y. Lin, G.-F. Xu, L. Zhao, Y.-N. Guo, Y. Guo, J. Tang, Dalton Trans., 40 (2011) 8213–8217.
(d) Y. Zhang, B. Ali, J. Wu, M. Guo, Y. Yu, Z. Liu, J. Tang, Inorg. Chem. DOI: 10.1021/acs.inorgchem.8b03249.
(e) A. K. Mondal, H. S. Jena, A. Malviya, S. Konar, Inorg. Chem. 55 (2016) 5237–5244.
(f) P. Zhang, L. Zhang, S. Y. Lin, S. Xue J. Tang, Inorg Chem. 52 (2013) 4587-92.
(g) H. F. Li, P. F. Yan, P. Chen, Y. Wang, H. Xu, G. M. Li, Dalton Trans. 41 (2012) 900-907.
(h) S. Y. Lin, L. Zhao, Y. N. Guo, P. Zhang, Y. Guo, J. Tang, Inorg Chem. 51 (2012) 10522-10528.
(i) X. A. Zhu, C. He, D. P. Dong, Y. Liu and C. Y. Duan, Dalton Trans.39 (2010) 10051-10055.
(j) C. Lincheneau, R. D. Peacock, T. Gunnlaugsson, Chem. Asian J. 5 (2010) 500-504.
(k) M. Albrecht, O. Osetska, R. Frohlich, J. C. G. Bunzli, A. Aebischer, F. Gumy, J. Hamacek, J. Am. Chem. Soc. 129 (2007) 14178-14179.
(l) C. D. B. Vandevyver, A. S. Chauvin, S. Comby, J. C. G. Bunzli, Chem. Commun. (2007) 1716-1719.
(m) F. Habib, J. Long, P. H. Lin, I. Korobkov, L. Ungur, W. Wernsdorfer, L. F. Chibotaru, M. Murugesu, Chem. Sci. 3 (2012) 2158−2164.
(n) B. E. Aroussi, S. Zebret, C. Besnard, P. Perrottet, J. Hamacek, J. Am. Chem. Soc. 133 (2011) 10764−10767.
(o) B. Wang, Z. Zang, H. Wang, W. Dou, X. Tang, W. Liu, Y. Shao, J. Ma, Y. Li, J. Zhou, Angew. Chem., Int. Ed. 52 (2013) 3756−3759.

[4] (a) G. Aromi, E. Brechin, Struct. Bonding, 122 (2006) 1 -67.
b) M. Andruh, J. P. Costes, C. Diaz, S. Gao, Inorg. Chem. 48 (2009) 3342–3359.
(b) C. Benelli, D. Gatteschi, Chem. Rev. 102 (2002) 2369–2388.
(c) T. R. Johannessen, G. Bernardinelli, Y. Filinchuk, S. Clifford, N. D. Favera, C. Piguet, Inorg. Chem. 48 (2009) 5512.
(d) M. Cantuel, F. Gumy, J. C. G. Bunzil, C. Piguet, Dalton Trans. (2006) 2647-2660.
(e) R. Sessoli, A. K. Powell, Coord. Chem. Rev. 253 (2009) 2328 -2341.
(f) L. Sorace , C. Benelli, D. Gatteschi, Chem. Soc. Rev. 40 (2011) 3092 -3104.
(g) S. Speed, F. Pointillart, J. C. Mulatier, L. Guy, S. Golhen, O. Cador, B. L. Guennic, F. Riobe, O. Maury, L. Ouahab, Eur. J. Inorg. Chem. 2017 (2017) 2100-2111.
(h) L. R. Piquer, E. C. Sañudo, Dalton Trans. 44 (2015) 8771-8780.
(i) D. I. Alexandropoulos, L. Cunha-Silva, G. Lorusso, M. Evangelisti, J. Tang, T. C. Stamatatos, Chem. Commun. 52 (2016) 1693-1696.

(j) E. Colacio, Mannich Base Ligands as Versatile Platforms for SMMs. In Topics in Organometallic Chemistry. Springer, Berlin, Heidelberg. (2018)

(k) C. Y. Chow, E. R. Trivedi, V. Pecoraro, C. M. Zaleski, Inorg Chem. 35 (2015) 214–253.

(l) K. Liu, W. Shi P. Cheng, Coord. Chem. Rev. 74-122 (2015) 289–290.

(m) M. Andruh, Dalton Trans., 44 (2015) 16633-16653

[5] D. Gatteschi , R. Sessoli, J. Villain, Molecular Nanomagnets, Oxford University Press, London, (2006).

[6] (a) L. Bogani W. Wernsdorfer, Nat. Mater 7 (2008) 179–186.

(b) M. Prezioso, A. Riminucci, P. Graziosi, I. Bergenti, R. Rakshit, R. Cecchini, A. Vianelli, F. Borgatti, N. Haag, M. Willis, A. J. Drew, W. P. Gillin, V. A. Dediu, Adv Mater. 25 (2013) 534–538.

(c) R.Vincent, S. Klyatskaya, M. Ruben, W. Wernsdorfer, F. Balestro, Nature 488 (2012) 357–360.

(d) M. Ganzhorn, S. Klyatskaya, M. Ruben, W. Wernsdorfer, Nat Nanotechnol. 8 (2013) 165–169.

(e) M. Jenkins, T. Hümmer, M. J. Martínez-Pérez, J. García-Ripoll, D. Zueco, F. Luis, New. J. Phys. 15 (2013) 095007.

(f) K. Katoh, H. Isshik,i T. Komeda, M. Yamashita, Chem. Asian. J. 7 (2012) 1154–1169.

(g) A. Cornia, A, P. Seneor, Nat. Mater. 16 (2017) 505–506.

(h) M. Affronte, J. Mater. Chem. 19 (2009) 1731–1737.

(i) R. Sessoli, M. E. Boulon, A. Caneschi, M. Mannini, L. Poggini, F. Wilhelm, A. Rogalev, Nat. Phys. 11 (2015) 69–74.

(j) M. N. Leuenberger, D. Loss, Nature 410 (2001) 789–793.

k) P. C. E. Stamp, A. Gaita-Ariño, J. Mater. Chem. 19 (2009) 1718–1730.

[7] (a) T. Gupta, M. F. Beg, G. Rajaraman, Inorg. Chem. 55 (2016) 11201–11215.

(b) S. K. Singh, M. F. Beg, G. Rajaraman, Chem. Eur. J. 22 (2016) 672–680.

(c) X. L. Li, F. Y. Min, C. Wang, S. Y. Lin, Z. Liu, J. Tang, Inorg. Chem. 54 (2015) 4337–4344

[8] (a) S. K. Langley, C. Le, L. Ungur, B. Moubaraki, B. F. Abrahams, L. F. Chibotaru, K. S. Murray, Inorg. Chem. 53 (2014) 8970–8978.

(b) S. K. Langley, D. P. Wielechowski, V. Vieru, N. F. Chilton, B. Moubaraki, B. F. Abrahams, L. F. Chibotaru, K. S. Murray, Angew. Chem. Int. Ed. 52 (2013) 12014–12019.

[9] C. Meseguer, S. Titos-Padilla, M. Hänninen, R. Navarrete, A. J. Mota, M. Evangelisti, J. Ruiz, E. Colacio, Inorg. Chem. 53 (2014) 12092-12099.

[10] E. Colacio, J. Ruiz, A. J. Mota, M. A. Palacios, E. Cremades, E. Ruiz, F. J. White, E. K. Brechin, Inorg. Chem. 51 (2012) 5857-5868.

[11] (a) M. Evangelisti, E. K. Brechin, Dalton. Trans. 39 (2010) 4672– 4676
(b) J. W. Sharples, D. Collison, Polyhedron 54 (2013) 91– 103
(c) R. Sessoli, Angew. Chem., Int. Ed. 51 (2012) 43– 45
(d) F. Luis, M. Evangelisti, In Molecular Nanomagnet and Related Phenomena; S. Gao, Ed.; Springer-Verlag: Berlin, Heidelberg, (2014) pp 431– 460.
(e) M. Evangelisti, In Molecular Magnets: Physics and Applications; J. Bartolomé, F. Luis, J. Fernández, Eds.; Springer-Verlag: Berlin, Heidelberg, (2014) pp 365– 385.
(f) J. L. Liu, Y. C. Chen, F. S. Guo, M. L. Tong, Coord. Chem. Rev. 281 (2014) 26– 49.

[12] APEX2; Bruker AXS: Madison, WI, (2010).

[13] SAINT, Version 8.30a; Bruker AXS: Madison, WI, (2013)

[14] G. M. Sheldrick, SADABS, Version 2004/1; Bruker AXS:Madison, WI, (2008).

[15] G. M. Sheldrick, Acta Crystallogr., Sect. A: Found. Crystallogr. 64 (2008) 112−122.

[16] O. V. Dolomanov, J. Bourhis, R. J. Gildea, J. A. K. Howard, H. Puschmann, J. Appl. Crystallogr. 42 (2009) 339−341.

[17] (a) S. Alvarez, P. Alemany, D. Casanova, J. Cirera, M. Llunell, D. Avnir, Coord. Chem. Rev. 249 (2005) 1693-1708,
(b) J. Cirera, E. Ruiz, S. Alvarez, Organometallics, 24 (2005) 1556-1562.

[18] N. F. Chilton, R. P. Anderson, L. D. Turner, A. Soncini and K. S. Murray, J. Comput. Chem., 34 (2013) 1164–1175.

[19] E. Colacio, J. Ruiz, A. J. Mota, M. A. Palacios, E. Cremades, E. Ruiz, F. J. White, E. K. Brechin, Inorg. Chem. 51 (2012) 5857-5868.

[20] J. P. Costes, F. Dahan, A. Dupuis, J. P. Laurent, Inorg. Chem. 36 (1997) 4284-4286

[21] T. D. Pasatoiu, J. P. Sutter, A. M. Madalan, F. Z. C. Fellah, C. Duhayon, M. Andruh, Inorg. Chem. 50 (2011) 5890-5898.

[22] M. Towatari, K. Nishi, T. Fujinami, N. Matsumoto, Y. Sunatsuki, M. Kojima, N. Mochida, T. Ishida, N. Re, J. Mrozinski, Inorg. Chem. 52 (2013) 6160−6178.

[23] J. P. Costes, L. Vendier, Eur. J. Inorg. Chem. (2010) 2768-2773.

[24] A. Chakraborty, P. Bag, E. Riviere, T. Mallah, V. Chandrasekhar, Dalton Trans. 43 (2014) 8921−8932.

[25] J. P. Costes, F. Dahan, L. Vendier, S. Shova, G. Lorusso, M. Evangelisti, Dalton Trans. 47 (2018) 1106–1116.

[26] J. P. Costes, S. Mallet-Ladeira, L. Vendier, R. Maurice, W. Wernsdorfer, Dalton

Trans. 48 (2019) 3404–3414.

[27] Q. W. Xie, S. Q. Wu, C. M. Liu, A. L. Cui, H. Z. Kou, Dalton Trans. 42 (2013) 11227–11233.

[28] J. M. Soler, E. Artacho, J. D. Gale, A. Garcia, J. Junquera, P. Ordejon, D. J. Sanchez-Portal, Phys.: Condens. Matter. 14 (2002) 2745-2779.

[29] J. P. Perdew, K. Burke, M. Ernzerhof, Phys. Rev. Lett. 77 (1996) 3865-3868.

[30] L. Kleinman, D. M. Bylander, Phys. Rev. Lett. 48 (1982) 1425-1428

[31] N. Troullier, N. J. L. Martins, Phys. Rev. B 43 (1991) 1993-2006.

[32] R. Pollet, D. J. Marx, Chem. Phys. 126 (2007) 181102.
[33] E. Ruiz, S. Alvarez, J. Cano, V. J. Polo, Chem. Phys. 123 (2005) 164110.

[34] V. Ruiz, A. Rodríguez-Fortea, J. Tercero, T. Cauchy, C. Massobrio, J. Chem. Phys. 123 (2005) 74102.

[35] E. Ruiz, P. Alemany, S. Alvarez, J. Cano, J. Am. Chem. Soc. 119 (1997) 1297-1303.

[36] (a) C. Benelli, D. Gatteschi, Chem. Rev. 102 (2002) 2369-2388 and references therein.
(b) J. P. Sutter, M. L. O Kahn, Magnetism: Molecules to Materials, J. S. Miller, M. Drillon, Eds., Wiley-VCH, Weinheim (2005) vol. V, p. 161-187
(c) E. Colacio, M. A. Palacios, A. Rodríguez-Diéguez, A. J. Mota, J. M. Herrera, D. Choquesillo-Lazarte, R. Clérac, Inorg Chem. 49 (2010) 1826-1833.

[37] (a) J. Ruiz, A. J. Mota, A. Rodríguez-Diéguez, S. Titos, J. M. Herrera, E. Ruiz, E. Cremades, J. P. Costes, E. Colacio, Chem. Commun. 48 (2012) 7916–7918.
(b) Y. Bi, Y. N. Guo, L. Zhao, Y. Guo, S. Y. Lin, S. D. Jiang, J. Tang, B. W. Wang, S. Gao, Chem. Eur. J. 17 (2011) 12476– 12481.
(c) H. L. C. Feltham, Y. Lan, F. Klöwer, L. Ungur, L. F. Chibotaru, A. K. Powell, S. Brooker, Chem. Eur. J. 17 (2011) 4362–4365.

[38] (a) J. P. Costes, L. Vendier, W. Wernsdorfer, Dalton Trans. 40 (2011) 1700-1706.
(b) E. Colacio, J. Ruiz, A. J. Mota, M. A. Palacios, E. Ruiz, E. Cremades, M. M. Hanninen, R. Sillampaa, E. K. Brechin, C. R. Chimie, 15 (2012) 878-888.

[39] J. P. Costes, F. Dahan, J. Garcia-Tojal, Chem. Eur. J. 8 (2002) 5430-5434.